https://doi.org/10.5194/egusphere-2025-6521
Preprint. Discussion started: 28 January 2026

Tropical belt expansion and its impacts on climate variability in the Mediterranean from 1980 to 2022

Mohamed Darrag[1], Shuanggen Jin[2,3*], Andres Calabia[4], Aalaa Samy[5], Ivan Radevski[6], and Ali M. Radwan[1]

[1]Geodynamic Department, National Research Institute of Astronomy and Geophysics-NRIAG, 11421 Helwan, Cairo, Egypt.
[2]School of Surveying and Land Information Engineering, Henan Polytechnic University, Jiaozuo 454003, China.
[3]School of Artificial Intelligence, Anhui University, Hefei 230601, China.
[4]Department of Physics and Mathematics, University of Alcala, 28801, Alcalá de Henares, Spain.
[5]Geomagnetic and Geoelectric Department, National Research Institute of Astronomy and Geophysics-NRIAG, 11421 Helwan, Cairo, Egypt.
[6]Institute of Geography, Faculty of Natural Sciences and Mathematics, Ss. Cyril and Methodius University, Skopje, North Macedonia

*Corresponding author: sgjin@hpu.edu.cn

Abstract.

The Mediterranean region's climatic parameters are undergoing substantial changes driven by climate change and tropical belt expansion. This paper explores the long-term variability of climatic parameters over the Mediterranean region and their relationship with tropical belt expansion by employing observational and reanalysis data from January 1980 to December 2022 through multiple approaches including correlation, linear regression, singular value decomposition (SVD), wavelet coherence (WTC), and principal component analysis (PCA). The lapse rate tropopause height (LRT-H) exhibits upward trends of approximately 80.58 m/dec. Concurrently, the tropical belt shows poleward expansion of approximately 0.14 °/dec and 0.27 °/dec from both applied methods. The tropical edge latitudes (TELs) of both applied approaches are in phase and have a strong positive correlation with LRT-H, surface temperature, and tropospheric temperature while being of strong negative correlation and out of phase with precipitation. However, there is no substantial correlation for the Standardized Precipitation Evapotranspiration Index (SPEI) with TELs or other climatic parameters. The results of SVD analysis depict that the surface temperature and lower tropospheric temperature (TRP-1) have evident coupling with the TELs in the eastern Mediterranean. Furthermore, surface temperature and TRP-1 have significant increasing trends, which are abundant in the eastern and northern Mediterranean. On the other hand, both precipitation and SPEI exhibit downward trends. Over the Mediterranean, an apparent spatial and temporal variation of climatic parameters is observed. The results confirm the linkage between climatic parameters' variability, coherence, and covariability with the TELs variability patterns over the study area, especially in the eastern Mediterranean region.

Keywords Climate change · Mediterranean region · Tropical belt · Tropopause · Climatic parameters

1 Introduction

Despite the fact that greenhouse gases (GHGs) emissions in Mediterranean countries are generally modest, climate change has been documented at a magnitude that exceeds global averages (Lange, 2020). The Mediterranean region is situated in a transition zone between the North Africa arid

https://doi.org/10.5194/egusphere-2025-6521
Preprint. Discussion started: 28 January 2026

climate and Central Europe temperate and wet climate, and it is influenced by interactions between mid-latitude and tropical processes. This makes the Mediterranean region potentially sensitive to climate change (Lionello et al., 2006; Ulbrich et al., 2006; Urdiales-Flores et al., 2023). In fact, the Mediterranean region has experienced significant shifts of climate in the past (Luterbacher et al., 2006), and it has been highlighted as one of the most important "Hot-Spots" in climate change future projections (Giorgi, 2006). This region, which comprises a semi-enclosed sea and neighboring lands, has seen substantial shifts in climate patterns over the last several decades. These changes are corroborated by evidence from the Mediterranean region, which shows altered temperature trends, altering precipitation regimes, and an increase in the extreme weather events frequency and severity (Insua-Costa et al. 2022; Androulidakis et al. 2023; Yavaşlı and Erlat, 2024). Climate change in the Mediterranean basin has far-reaching implications that influence critical socioeconomic areas in addition to meteorological difficulties. These changes have significant implications for agriculture, water resource management, coastal zone planning, and the protection of sensitive ecosystems (Raihan 2023; Noto et al. 2023). Understanding and forecasting climatic patterns is crucial for developing effective adaptation strategies and making informed policy decisions in a highly reactive region to reduce climate change effects (Mastrorillo et al., 2024).

In astronomy and cartography, the Tropics of Cancer and Capricorn, at latitudes of ~23.5º north and south define the tropical belt's boundaries (Gnanadesikan and Stouffer, 2006). While in climatology the tropical edge latitudes (TELs) vary seasonally, and in response to climate forcing. They migrate poleward in the summer and equatorially in the winter (Davis and Birner, 2013). Tropical belt expansion has been robustly detected across the globe using a variety of data sets and approaches (Lucas et al., 2014). The expansion of the tropical belt has been attributed to several factors, including tropospheric warming caused by GHGs forcing, stratospheric cooling owing to ozone depletion, sea-surface temperature (SST) variability over the tropics, in addition to the absorbing aerosols hemispheric asymmetry (Seidel et al. 2008; Allen et al. 2012, 2014; Grise et al. 2018). The sixth Assessment Report (AR6) of the Intergovernmental Panel on Climate Change (IPCC) shows that Hadley circulation (tropics) is expanding poleward at a rate of approximately 0.5-1° per decade, with significant regional and seasonal variability (Mathew and Kumar, 2018; Staten et al. 2018). The expansion of the tropics could cause substantial changes in the global climate system; even slight expansion of the tropical belt could cause substantial changes in the global climate system, manifesting as altered precipitation patterns, poleward-shifting storm tracks and jet streams, variations in stratospheric trace gas distribution, and changes in ocean circulation (Seidel et al., 2008; Lucas et al., 2014).

The IPCC has repeatedly identified the Mediterranean as one of the most vulnerable regions to the effects of climate change (IPCC, 2021a,b). One of the primary drivers of this susceptibility is the expansion of the tropical belt, which has a significant impact on subtropical and mid-latitude climates (Seidel et al., 2008). The Mediterranean basin is tropicalizing, with its waters increasing warmer and saltier. The enclosed sea warms four times quicker than the global norm for coastal

https://doi.org/10.5194/egusphere-2025-6521
Preprint. Discussion started: 28 January 2026

waters (Bianchi and Morri, 2003; Borghini et al., 2014), and it is anticipated that these rates will rise throughout this century as climate change progresses (Somot et al., 2006; Rilov and Galil, 2009). The widening of the tropical belt has direct implications for precipitation patterns, temperature regimes, and the frequency of extreme weather events in the Mediterranean. As the subtropical dry zones move poleward, the Mediterranean region experiences longer droughts, lower rainfall, and more intense heatwaves (Giorgi, 2019). These changes impair agricultural production, water availability, and ecosystem stability, worsening socioeconomic vulnerability (Lionello et al., 2006). Furthermore, Mediterranean Sea warming alters marine biodiversity and accelerates tropical species migration, threatening native ecosystems and fisheries. Desertification processes, driven by decreased soil moisture and increased evapotranspiration, strain terrestrial ecosystems and impede sustainable development in the region (Cramer et al., 2018).

The Mediterranean region has experienced major variations in climatic parameters during recent decades. Its unique geographical position, bounded by Europe, North Africa, and the Middle East, makes it particularly vulnerable to global warming and climate variability impacts (Giorgi, 2006). Climate models and observational data consistently indicate that the Mediterranean basin is warming at a rate higher than the global average (Lionello et al., 2012). The region has warmed by approximately 1.4°C since the late 19th century, exceeding the global mean temperature rise of 1.1°C (Cramer et al., 2018). This accelerated warming has increased the frequency and intensity of heatwaves, with profound impacts on human health, agriculture, and biodiversity (Kuglitsch et al., 2010). Over the Mediterranean region, precipitation is distributed unevenly throughout the year, with a significant decline in the warm season. The region is also recognized for its wide spatial and temporal variation in precipitation levels (Lionello et al., 2006; Vicente-Serrano et al., 2025). Shifts in precipitation patterns have also been observed across the Mediterranean. Projections indicate that precipitation could decline by 10-30% by the end of the 21st century, exacerbating drought conditions and increasing water scarcity (Gao and Giorgi, 2008).

Understanding the interplay between tropical belt expansion and regional climate variability is essential for developing adaptive strategies to mitigate the adverse effects of climate change in the Mediterranean. This paper explores the multifaceted impacts of tropical expansion on Mediterranean climate. Section 2 describes the datasets used and methods for deriving tropical edge latitudes. Section 3 presents the analysis results, and Section 4 provides our conclusions.

2 Data and methods

2.1 Study area

The Mediterranean region encompasses areas surrounding the Mediterranean Sea, including parts of Southern Europe, North Africa, and the Middle East. In this work, the study region is defined as the area between 20° N and 50° N latitude and 15° W and 50° E longitude. The Mediterranean basin is characterized by substantial environmental and geographical gradients, complex morphology with mountain chains and significant land-sea contrasts, and location in a transition zone between mid-latitude and subtropical atmospheric circulation systems, contributing to its

https://doi.org/10.5194/egusphere-2025-6521
Preprint. Discussion started: 28 January 2026

complex climate patterns (Lange, 2020). The Mediterranean region is recognized as a climate change hotspot due to its unique geographic, climatic, ecological, and socio-economic characteristics. Its semi-enclosed nature amplifies warming and limits the exchange of heat and moisture with surrounding regions, making it particularly vulnerable to climate change. The region is warming approximately 20% faster than the global average, leading to profound changes in temperature and precipitation patterns (Cramer et al., 2018). Projections indicate marked increases in heatwaves, droughts, and extreme rainfall events, intensifying challenges for water resources, agriculture, and biodiversity (IPCC, 2021a). The Mediterranean basin hosts one of the world's richest biodiversity reserves with numerous endemic species; however, rising temperatures, habitat loss, and changing phenological patterns pose significant threats (Coll et al., 2010; Lionello et al., 2012). The socio-economic consequences are equally profound, affecting tourism, fisheries, agriculture, and urban settlements, while sea level rise threatens coastal infrastructure and ecosystems (IPCC, 2021a).

2.2 Data

This study utilizes multiple datasets spanning January 1980 to December 2022 to investigate climate variability in the Mediterranean region. Monthly averaged temperature data on pressure levels from ERA5, the fifth generation ECMWF reanalysis, are used to determine lapse rate tropopause (LRT) parameters (height and temperature). ERA5 provides data at 0.25° × 0.25° horizontal resolution (approximately 31 km × 31 km) with 37 vertical pressure levels ranging from 1,000 hPa to 1 hPa (Hersbach et al., 2019a). Monthly averaged surface temperature and total precipitation data are also obtained from ERA5 at 0.25° × 0.25° resolution (Hersbach et al., 2019b) to explore the impacts of tropical belt expansion on temperature and precipitation patterns over the Mediterranean region. Additionally, monthly precipitation and potential evapotranspiration (PET) data at 0.5° × 0.5° resolution from the Climatic Research Unit (CRU) Time-Series (Harris et al., 2020) are used to compute the Standardized Precipitation Evapotranspiration Index (SPEI) as a meteorological drought indicator, following the methodology of Vicente-Serrano et al. (2010) and Beguería et al. (2013).

2.3 Methods

We apply the LRT definition to determine tropopause parameters (height and temperature) using ERA5 temperature data on pressure levels. Temperature data are first vertically interpolated to a regular 100 m height resolution (Hindley et al., 2015). Following the WMO definition, the thermal LRT is identified as the lowest level at which the lapse rate decreases to 2°C/km or less, provided the average lapse rate between this level and all higher levels within 2 km does not exceed 2°C/km (WMO, 1957). Long-term trends of tropopause parameters over the Mediterranean region from January 1980 to December 2022 are examined using linear regression analysis at all grid points. The TEL, which indicates tropical belt width, is estimated using two tropopause height metrics. The first method defines TEL as the latitude at which LRT height (LRT-H) drops 1.5 km below

https://doi.org/10.5194/egusphere-2025-6521
Preprint. Discussion started: 28 January 2026

the tropical average (15°S-15°N) (Birner, 2010; Davis and Rosenlof, 2012) and it can be abbreviated as TPD. The second method defines TEL as the latitude of maximum LRT-H meridional poleward gradient (Davis and Rosenlof, 2012; Davis and Birner, 2017) and it can be abbreviated as TPG. Tropical belt expansion rates are determined using both methods.

The relationships between TEL and climatic parameters are examined through multiple statistical approaches: correlation analysis, linear regression, singular value decomposition (SVD), wavelet coherence (WTC), and principal component analysis (PCA) (Minh et al., 2024). We investigate the connection between tropical expansion and tropopause characteristics, surface temperature (both as a driver of and response to tropical belt changes), tropospheric temperature (from Earth's surface to the LRT level), precipitation, and SPEI as a meteorological drought indicator. WTC analysis illustrates the time-frequency relationships between TEL positions from both methods and climatic parameters. WTC estimates coherence between two time series within the time-frequency space, with values ranging from 0 to 1 (Grinsted et al., 2004). SVD analysis identifies coupled modes of covariability between TEL locations and climatic parameters. This technique recognizes pairs of coupled spatial patterns and their temporal variations, with each pair describing a fraction of the covariance between fields. The temporal cross-covariance matrix is constructed between the two space- and time-dependent data fields, which need not have the same number of grid points but must span the same time period (Bjornsson and Venegas, 1997; Darrag et al., 2024). Before performing the SVD analysis, all employed variables were pre-processed to remove the long-term trend and the seasonal cycles because we're not interested in seasonal signals. This detrending and deseasonalization is necessary, as removing these components ensures that the SVD analysis results primarily capture covariability between the TELs and the climatic parameters.

3 Results and discussion

3.1 Tropopause and tropical belt characteristics

The monthly average of LRT parameters (height and temperature) over the period from January 1980 to December 2022 is depicted in Figure 1 top. Our analysis reveals that LRT-H has increased by approximately 80.58 ± 3.07 m/dec since January 1980 (Fig. 1a), consistent with Schmidt et al. (2008), who reported a global upward trend in LRT-H of 39 to 66 m/dec. This tropopause height increase is attributed to global warming driven by increasing atmospheric GHG concentrations (Meng et al., 2021). Our findings align with previous studies documenting global tropopause height increases from GNSS-RO data (Darrag et al., 2022), radiosonde observations (Seidel and Randel, 2006), and reanalysis datasets (Santer et al., 2004). LRT-T exhibits a downward trend of -0.12 ± 0.02 K/dec (Fig. 1b), with LRT-H showing a strong negative correlation of -0.86 with LRT-T. These LRT parameter trends are consistent with earlier research (Schmidt et al., 2004; Sausen and Santer, 2003; Seidel and Randel, 2006; Pisoft et al., 2021).

Tropopause parameters exhibit significant anomalies driven by atmospheric dynamics, climate change, and natural variability. The anomaly of tropopause parameters over the period January

https://doi.org/10.5194/egusphere-2025-6521
Preprint. Discussion started: 28 January 2026

1980 to December 2022 is shown in Figure 1 middle. LRT-H displays stronger positive anomalies than negative ones, with the maximum positive anomaly of approximately 1.67 km occurring in September 2020 and the greatest negative anomaly of approximately -1.22 km in April 1982. Positive anomalies dominate during summer and autumn, while negative anomalies dominate during winter and spring (Fig. 1c). Conversely, LRT-T exhibits stronger negative anomalies than positive ones, with a maximum positive anomaly of approximately 3.4 K in April 1990 and a greatest negative anomaly of approximately -3.62 K in September 2000. In contrast to LRT-H, LRT-T positive anomalies dominate during winter and spring, while negative anomalies dominate during summer and autumn (Fig. 1d). The anomalies of both tropopause parameters are dominated by inter-annual oscillations and vary across different months. Our results are consistent with Seidel and Randel (2006), who reported tropopause monthly anomalies with standard deviations (SDs) ranging between 0.2 and 0.6 km for LRT-H.

Linear regression analysis of LRT parameters was performed at all grid points, with decadal trends plotted in Figure 1 bottom. LRT-H shows a dominant upward trend evident across almost the entire study area, with statistically significant trends at $p < 0.05$ at most of the grid points (Fig. 1e). The eastern Mediterranean region around 30° N exhibits the maximum LRT-H increasing trends, reaching 266.5 m/dec, attributed to the stronger influence of the South Asian monsoon system in this area (Tyrlis and Lelieveld, 2013). The zonal mean of the LRT-H regression map (right panel of Figure 1e) indicates increasing trends at all latitudes, with the latitudinal band between 30° N and 33.75° N showing maximum upward trends. For LRT-T (Fig. 1f), the majority of the study area displays decreasing trends with statistically significant values at $p < 0.05$ at most of the grid points. The LRT-T regression map reveals a spatial pattern opposite to that of LRT-H, consistent with previous studies (Darrag et al., 2022, 2024). The greatest LRT-T downward trend occurs in the eastern Mediterranean region around 30° N, with maximum decreasing trends of approximately -0.75 K/dec. The zonal mean of the LRT-T regression map (right panel of Figure 1f) shows decreasing trends at all latitudes except the northern zone of the Mediterranean region between 43.5° N and 50° N, with the latitudinal band from 20° N to 32.25° N exhibiting maximum downward trends.

In this study, TEL representing the tropical belt boundary over the Mediterranean region is estimated using two tropopause height metrics. Figure 2 depicts TEL derived from ERA5 data based on both TPD and TPG methods over the period from January 1980 to December 2022. The TPD method shows an observed increase in tropical belt coverage of approximately 0.14 ± 0.05 °/dec (Fig. 2a). The TPG method exhibits more poleward TEL occurrences than the TPD method. Tropical belt coverage expanded by approximately 0.27 ± 0.06 °/dec using the TPG method (Fig. 2b). Meng et al. (2021) reported that the latitudinal zone from 30° N to 40° N exhibits the largest LRT-H trends, likely attributable to the poleward shift of the subtropical jet and tropical belt widening over the past 40 years (Staten et al., 2018). The TPD TEL demonstrates a strong positive association with LRT-H, with a linear regression model yielding a coefficient of determination

https://doi.org/10.5194/egusphere-2025-6521
Preprint. Discussion started: 28 January 2026

(R^2) of 0.93 (Fig. 2c). Similarly, the TPG TEL exhibits a strong positive association with LRT-H, with $R^2 = 0.87$ (Fig. 2d).

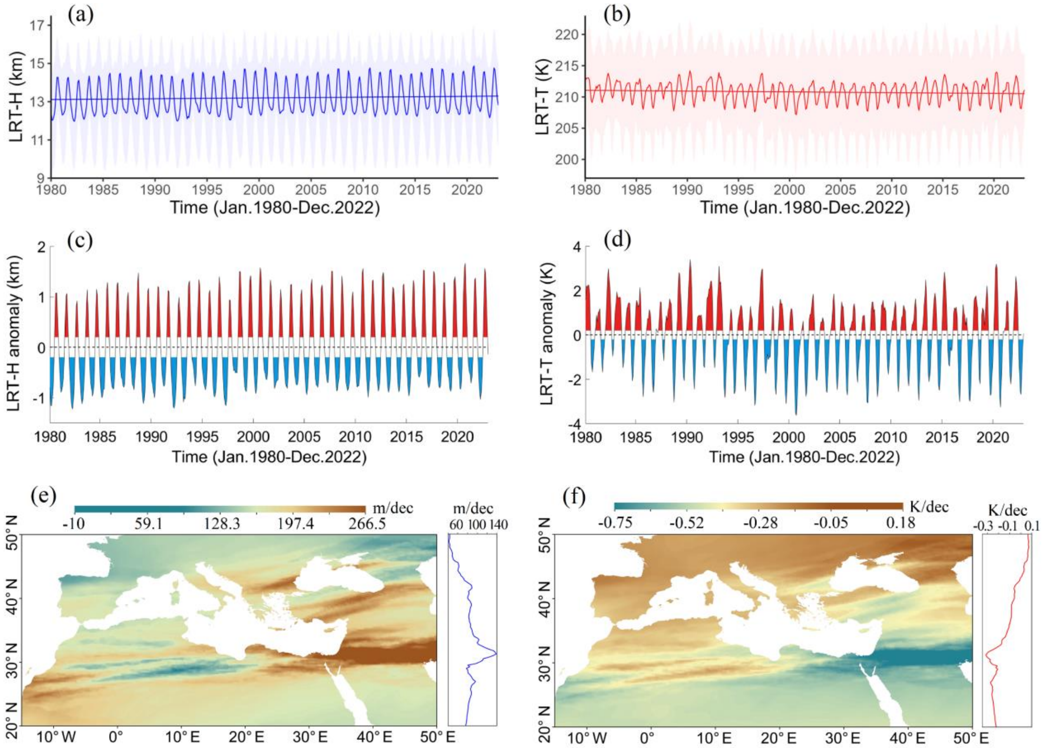

Figure 1. Monthly time series of LRT parameters from January 1980 to December 2022 in the top: (a) tropopause height (LRT-H), (b) tropopause temperature (LRT-T). Tropopause anomaly over the period January 1980 to December 2022 in the middle: (c) LRT-H anomaly time series, (d) LRT-T anomaly time series. Linear regression analysis of LRT parameters at all grid points and their decadal trends over the period January 1980 to December 2022 in the bottom: (e) LRT-H, (f) LRT-T. The zonal mean is displayed on the right side of each regression map.

The longitudinal variation of TEL for both approaches over the Mediterranean region from January 1980 to December 2022 is depicted in Figure 2e,f. Both the TPD TEL (Fig. 2e) and TPG TEL (Fig. 2f) display clear longitudinal variation across the study area. For both methods, TEL in the eastern Mediterranean is positioned more poleward than in the western Mediterranean. This pattern results from multiple factors, including the eastern Mediterranean region's exposure to strong natural climate fluctuations connected to major tropical systems (Alpert et al., 2005). Furthermore, the Mediterranean region's dual climate influence (situated between the subtropical high-pressure systems of the Hadley cell and the mid-latitude westerlies) causes longitudinal differences in TEL through variations in these circulation patterns (Trigo et al., 2006). The contrast between the cooler waters of the western Mediterranean and the warmer landmasses of North Africa and the Middle East contributes to longitudinal TEL variations, with this contrast being more pronounced in the eastern Mediterranean, resulting in higher TEL values in this region (Lionello, 2012). Additionally, SST variability influences longitudinal TEL variation, as SST patterns affect atmospheric

https://doi.org/10.5194/egusphere-2025-6521
Preprint. Discussion started: 28 January 2026

circulation and climate boundary positions (Meli et al., 2023). As shown in Figure 2, TEL variability in the TPG method (Fig. 2f) is higher than in the TPD method (Fig. 2e). Moreover, the TPG TEL occurrences are more poleward, with a maximum value of approximately 42.88° N, compared to the TPD TEL maximum of approximately 42.78° N.

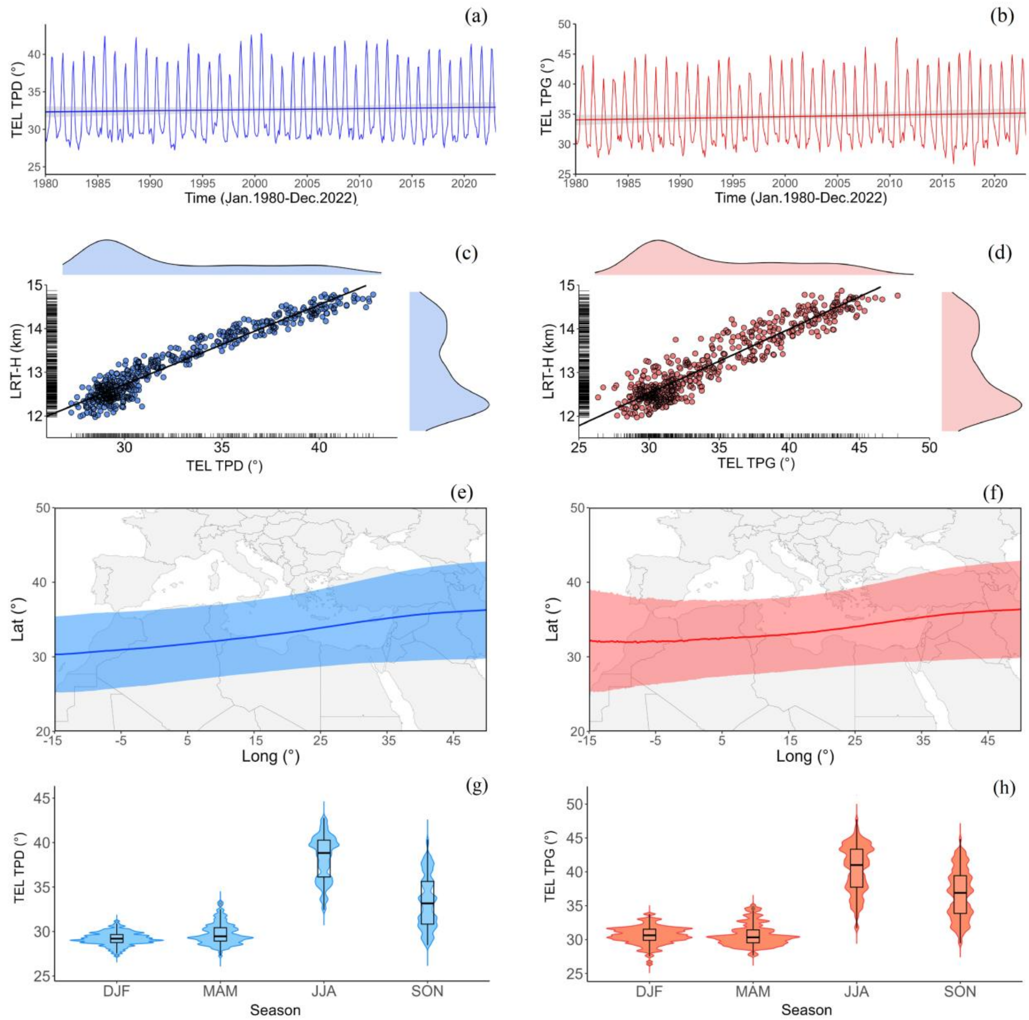

Figure 2. Monthly time series of the TPD TEL method over the Mediterranean region for the period January 1980 to December 2022 (a) and monthly time series of the TPG TEL method over the Mediterranean region for the period January 1980 to December 2022 (b). The linear regression model between TPD TEL and LRT-H (c) and the linear regression model between TPG TEL and LRT-H (d) is also presented. Longitudinal variation of TEL using both methods over the Mediterranean region from January 1980 to December 2022. The blue line in (e) represents the mean TPD TEL at each longitude over the study period, while the blue shading depicts its standard deviation (SD). In (f), the red line represents the mean TPG TEL at each longitude over the study period, with the red shading indicating its standard deviation (SD). Seasonal variation of TPD TEL (g) and TPG TEL (h) over the period from January 1980 to December 2022.

https://doi.org/10.5194/egusphere-2025-6521
Preprint. Discussion started: 28 January 2026

Figures 2g and 2h depict the seasonal variation of both TPD TEL and TPG TEL over the period from January 1980 to December 2022, respectively. In the case of TPD TEL, Summer (JJA) and Autumn (SON) show higher interannual variability than that in Winter (DJF) and Spring (MAM) (Fig. 2g). The TPD TEL median values exhibit the anticipated seasonal pattern, being maximum in Summer (JJA) at about 38.83° due to warming in the surface and troposphere. On the other hand, the TPD TEL median is minimum in Winter (DJF) at about 29.2° because of the cooling of the surface and troposphere. All seasons show a multimodal distribution of the TPD-TEL, which is clearly evident in Summer (JJA) and Autumn (SON). For TPG TEL (Fig. 2h), the seasonal variation follows the same pattern as that of TPD TEL, being of higher variability in Summer (JJA) and Autumn (SON) than in Winter (DJF) and Spring (MAM), displaying multimodal distribution of the TPG TEL values in all seasons. But TPG TEL exhibits TEL median values that are higher than those in the case of TPD TEL, being greatest in Summer (JJA) at about 41° and lowest in Spring (MAM) instead of Winter (DJF) in the case of TPD TEL, at about 30.33°. Our analysis results are consistent with those of several researches that reported a pronounced seasonal cycle of the TELs that typically moves poleward in the Summer and equatorward in the Winter. In addition, the amplitude of the seasonal cycle is approximately 5-10° latitude, though it varies depending on the metric employed (Davis and Rosenlof, 2012; Davis and Birner, 2013; Lucas et al., 2014; Luan et al., 2020).

3.2 Interaction of TEL and climatic parameters

Tropical belt expansion may cause profound changes in the Mediterranean region's climate; even minor expansion would have significant consequences. As shown in Figure 3, TELs estimated using both TPD and TPG methods exhibit a high Pearson correlation of 0.9. Furthermore, TELs from both definitions show strong correlations with LRT-H, surface temperature, tropospheric temperature, and precipitation. The TPD method demonstrates higher correlations with these climatic parameters than the TPG method. Correlations between TPD TEL and LRT-H, surface temperature, tropospheric temperature, and precipitation are 0.94, 0.78, 0.66, and -0.67, respectively. Our analysis results are consistent with those of Darrag et al. (2023). Additionally, tropospheric temperature depicts a strong correlation with surface temperature of approximately 0.97. However, no significant correlation exists between SPEI and all other climatic parameters. As shown in Figure 3, TEL from both definitions, LRT-H, surface temperature, and tropospheric temperature display bimodal distributions, while precipitation and SPEI exhibit unimodal distributions. TPD and TPG TEL show strong positive linear associations with LRT-H, surface temperature, and tropospheric temperature. Furthermore, tropospheric temperature demonstrates strong associations with other parameters, with the strongest relationship observed with surface temperature. Both precipitation and SPEI display negative associations with all other parameters while exhibiting a weak positive association with each other.

https://doi.org/10.5194/egusphere-2025-6521
Preprint. Discussion started: 28 January 2026

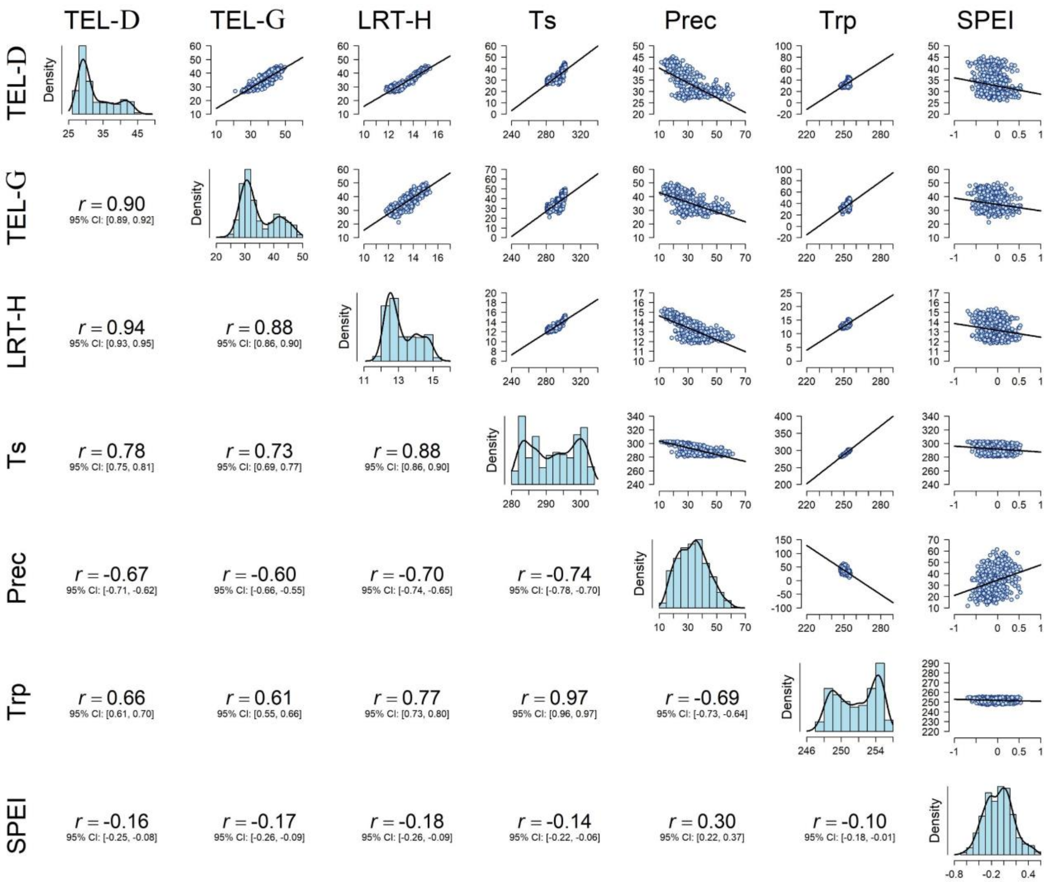

Figure 3. Correlation coefficients among monthly TEL from TPD (D) and TPG (G) methods, LRT-H, surface temperature (Ts), precipitation (Prec), tropospheric temperature (TRP), and SPEI with 95% confidence intervals for the period from January 1980 to December 2022 (left side). The density distribution of all variables is displayed on the diagonal, while linear regression models between variables are shown on the right side.

The PCA biplot of monthly averaged TEL from TPD and TPG methods, LRT-H, surface temperature, precipitation, tropospheric temperature, and SPEI (Fig. 4) reveals that TELs from both methods are highly positively correlated. Furthermore, the TPD TEL contributes more to variability than the TPG TEL. LRT-H, surface temperature, and tropospheric temperature are highly correlated with each other and with both TEL definitions. Conversely, precipitation and SPEI are weakly positively related. Precipitation shows negative correlations with TELs from both methods, LRT-H, surface temperature, and tropospheric temperature. Furthermore, SPEI depicts no observable relationship with TELs or other climatic parameters, showing high agreement with results in Figure 3. WTC analysis between TPD TEL and climatic parameters (LRT-H, surface temperature, tropospheric temperature, precipitation, and SPEI) is presented in Figure 5. Over the period from January 1980 to December 2022, TEL locations are in phase and exhibit high coherence with LRT-H, surface temperature, and tropospheric temperature at time scales of 4 to

https://doi.org/10.5194/egusphere-2025-6521
Preprint. Discussion started: 28 January 2026

20 months, 8 to 20 months, and 8 to 20 months, respectively. In relation to LRT-H, surface temperature, and tropospheric temperature, TEL is leading, as indicated by arrows pointing to the right and upward (Fig. 5a,b,c). Conversely, TPD TEL and precipitation show coherence at a time scale of 8 to 16 months, are out of phase, and TPD TEL is lagging (Fig. 5d). Furthermore, no significant coherence exists between TPD TEL and the SPEI drought index (Fig. 5e). As shown in Figure 6, WTC analysis results between TPG TEL and climatic parameters (LRT-H, surface temperature, tropospheric temperature, precipitation, and SPEI) are nearly identical to those of TPD TEL (Fig. 5) but with shorter time scales of high coherence. Our analysis outputs are consistent with Darrag (2024), who applied similar analyses in both hemispheres based on TELs estimated from global navigation satellite systems radio occultation (GNSS-RO) data on a global scale.

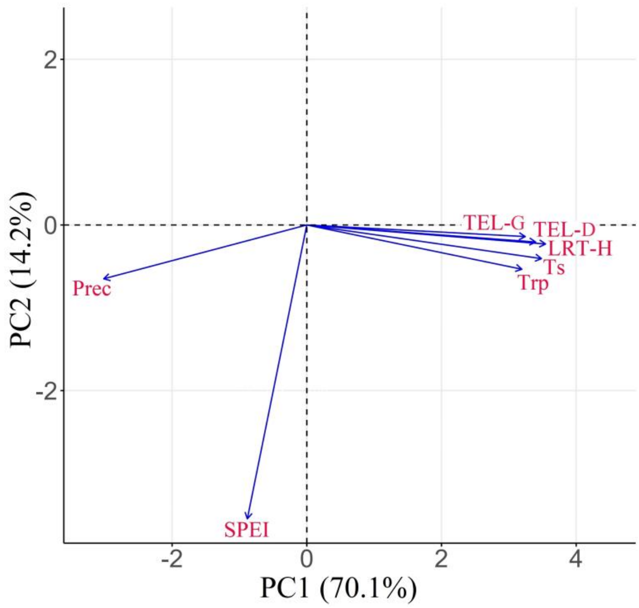

Figure 4. PCA biplot of monthly TEL from TPD (D) and TPG (G) methods, LRT-H, surface temperature (Ts), precipitation (Prec), tropospheric temperature (TRP), and SPEI for the period January 1980 to December 2022.

https://doi.org/10.5194/egusphere-2025-6521
Preprint. Discussion started: 28 January 2026

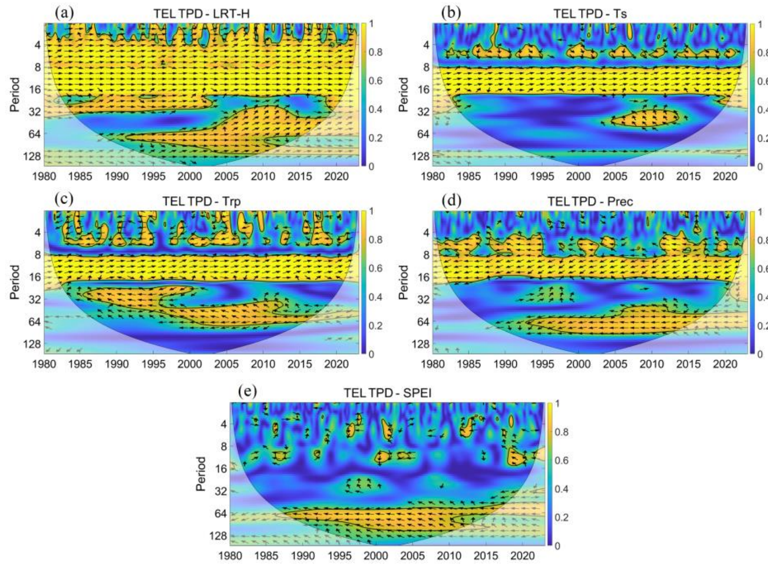

Figure 5. Wavelet coherence (WTC) analysis between TPD TEL and climatic parameters for the period from January 1980 to December 2022. Arrows indicate phase differences between the two series. Variables are in phase when arrows point to the right (moving in the same direction with cyclical effects on each other). If arrows point right and upward, the first variable is leading (causing the second variable); if pointing right and downward, the first variable is lagging. Variables are out of phase (having anticyclical effects) when arrows point to the left. If arrows point left and upward, the first variable is leading; if pointing left and downward, the first variable is lagging. TPD TEL and LRT-H (a), TPD TEL and surface temperature (Ts) (b), TPD TEL and tropospheric temperature (TRP) (c), TPD TEL and precipitation (Prec) (d), and TPD TEL and SPEI (e).

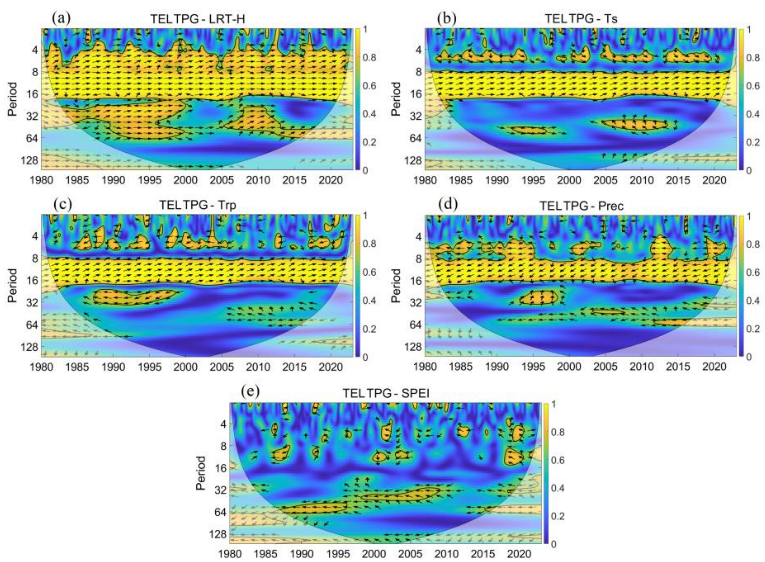

Figure 6. Wavelet coherence (WTC) analysis between TPG TEL and climatic parameters for the period from January 1980 to December 2022. TPG TEL and LRT-H (a), TPG TEL and surface temperature (Ts) (b), TPG TEL and tropospheric temperature (TRP) (c), TPG TEL and precipitation (Prec) (d), and TPG TEL and SPEI (e).

https://doi.org/10.5194/egusphere-2025-6521
Preprint. Discussion started: 28 January 2026

Figure 7 exhibits the spatial correlation of both TEL definitions with climatic parameters (surface temperature, lower tropospheric temperature from surface to 5 km height (TRP-1), upper tropospheric temperature from 5 km to LRT level (TRP-2), precipitation, and SPEI) from January 1980 to December 2022. As shown in Figure 7a,b, surface temperature displays positive correlations with TPD and TPG TEL definitions across the entire study area. The correlation reaches a maximum of approximately 0.92 over the eastern Mediterranean region. Similarly, TRP-1 exhibits positive correlations with both TEL definitions over all grid cells (Fig. 7c,d). The correlation is greatest over the eastern Mediterranean region, reaching approximately 0.88 for TRP-1 and TPD TEL. For TRP-2, positive correlations with TELs dominate and cover nearly the entire Mediterranean region (Fig. 7e,f), except the latitudinal band where TELs vary poleward and equatorward (Fig. 2e,f). The positive correlation of TRP-2 with TELs from both definitions reaches a maximum of approximately 0.95. Conversely, the greatest negative correlation between TRP-2 and TPG TEL is approximately -0.38. For precipitation, strong negative correlations with both TEL definitions dominate in the eastern Mediterranean region, reaching -0.75, while positive correlations cover North Africa and southern Europe but are weaker than the negative correlations in the eastern Mediterranean (Fig. 7g,h). SPEI shows weak correlations with both TPD and TPG TEL (Fig. 7i,j). Figure 7 demonstrates that the spatial correlation patterns of TEL from both definitions with climatic parameters are nearly identical. Our analysis results are in good agreement with the findings of Darrag (2024).

For further investigation into the effects of poleward tropical belt expansion on climatic parameters in the Mediterranean region from January 1980 to December 2022, SVD analysis is performed to reveal coupled patterns of covariability between TEL positions and climatic parameters (surface temperature, TRP-1, TRP-2, precipitation, and SPEI). First, we constructed 3D geospatial data using monthly TEL values by repeating TEL values along all longitudes for each timestep. This process was performed for both TPD and TPG TEL methods, resulting in 3D matrices for monthly TEL values in the same spatial and temporal domain as the climatic parameters. For the SVD analysis results, we consider only the first dominant mode of covariance. SVD1 depicts the spatial patterns for the first paired mode of covariability, whereas SC1 represents the time series of expansion coefficients for the same mode. For all parameters employed in the SVD examination, their SC1 time series and related SVD1 maps of spatial variability are scaled to range from -1 to 1 to enable comparison and description of the paired modes of covariability (Darrag et al., 2024).

For the coupled fields of TPD TEL and surface temperature, the squared covariance fraction (SCF) of the first leading mode explains 99.98% of the total covariability of both fields. As shown in Figure 8c, there is a strong positive correlation between the SC1 of TPD TEL and surface temperature of approximately 0.86. Furthermore, inter-annual oscillations dominate the SC1 for the temporal variability-paired mode of TPD TEL and surface temperature. The first coupled mode of spatial variability, SVD1, shows that surface temperature (Fig. 8b) is characterized by observed fluctuations in the eastern Mediterranean region accompanied by TPD TEL fluctuations of the same sign over the same region (Fig. 8a). For the coupled fields of TPD TEL and TRP-1, the SCF

https://doi.org/10.5194/egusphere-2025-6521
Preprint. Discussion started: 28 January 2026

of the first prevailing mode accounts for approximately 99.98% of the total covariability of both fields. As depicted in Figure 8f, there is strong coupling between the SC1 of TPD TEL and TRP-1 with a correlation of 0.88. Additionally, inter-annual oscillations dominate the SC1 for the temporal variability-paired mode of TPD TEL and TRP-1. The SVD1 exhibits that TRP-1 (Fig. 8e) is characterized by strong observed fluctuations in the eastern Mediterranean region and weak anomalies at the transition zone from low to mid-latitudes over Africa, accompanied by TPD TEL fluctuations of the same sign over the same region (Fig. 8d). For the coupled fields of TPD TEL and TRP-2, the SCF of the first dominant mode describes approximately 99.56% of the total covariability of both fields. As shown in Figure 8i, there is a strong correlation between the SC1 of TPD TEL and TRP-2 of approximately 0.89. Moreover, inter-annual oscillations dominate the SC1 for the temporal variability-paired mode of TPD TEL and TRP-2. The SVD1 depicts that TRP-2 (Fig. 8h) has clear coupling of the opposite sign with TPD TEL (Fig. 8g) in the southernmost part of Europe and the northernmost part of Africa, while in the southernmost part and the northernmost part of the study area both show fluctuations of the same sign.

In the case of the coupled fields of TPD TEL and precipitation, the SCF of the first leading mode explains approximately 99.71% of the total covariability of both fields. As exhibited in Figure 8l, there is a high correlation between the SC1 of TPD TEL and precipitation of approximately 0.8. Additionally, inter-annual oscillations dominate the SC1 for the temporal variability-paired mode of TPD TEL and precipitation. The SVD1 depicts that precipitation (Fig. 8k) is characterized by two narrow signals of strong fluctuations in the eastern Mediterranean region, one associated with TPD TEL fluctuations of the same sign and the other with TPD TEL fluctuations of opposite sign, and another two covariability zones in southern Europe of the same characteristics as that of the eastern Mediterranean region (Fig. 8j). For the coupled fields of TPD TEL and SPEI, the SCF of the first dominant mode represents approximately 97.17% of the total covariability of both fields. As shown in Figure 8o, the correlation between the SC1 of TPD TEL and SPEI is weaker than with other parameters, approximately 0.41. Moreover, inter-annual oscillations dominate the SC1 for the temporal variability-paired mode of TPD TEL and SPEI. The SVD1 depicts that SPEI (Fig. 8n) has clear coupling of the same sign with TPD TEL (Fig. 8m) in major areas of the eastern Mediterranean region and northern Africa, while in major areas of western Europe, both show fluctuations of opposite sign. The first leading mode of covariability for the coupled fields of TPG TEL and climatic parameters from January 1980 to December 2022 (Fig. 9) shows coupling patterns nearly identical to those for TPD TEL (Fig. 8). The SVD analysis results show that the patterns of combined TELs and climatic parameters are more closely coupled for surface temperature and TRP-1. Furthermore, their combined fields are significantly related in the eastern Mediterranean region, attributed to the more poleward TEL position in the eastern Mediterranean compared to the entire study area (Trigo et al., 2006; Lionello, 2012).

https://doi.org/10.5194/egusphere-2025-6521
Preprint. Discussion started: 28 January 2026

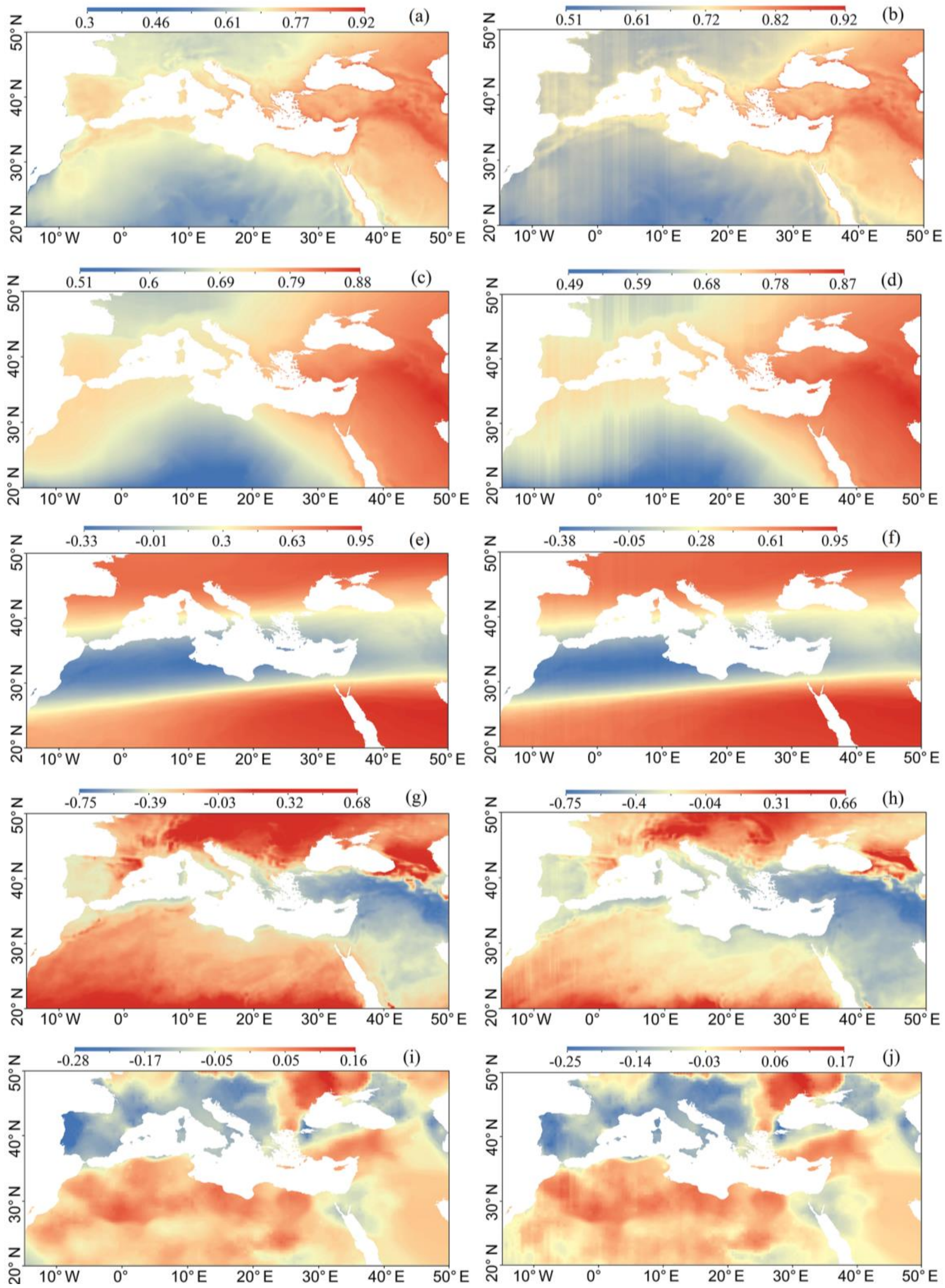

Figure 7. Spatial correlation of TPD TEL (left) and TPG TEL (right) with climatic parameters from January 1980 to December 2022. Surface temperature (a, b), lower tropospheric temperature from surface to 5 km height (TRP-1) (c, d), upper tropospheric temperature from 5 km to LRT level (TRP-2) (e, f), precipitation (g, h), and SPEI (i, j).

https://doi.org/10.5194/egusphere-2025-6521
Preprint. Discussion started: 28 January 2026

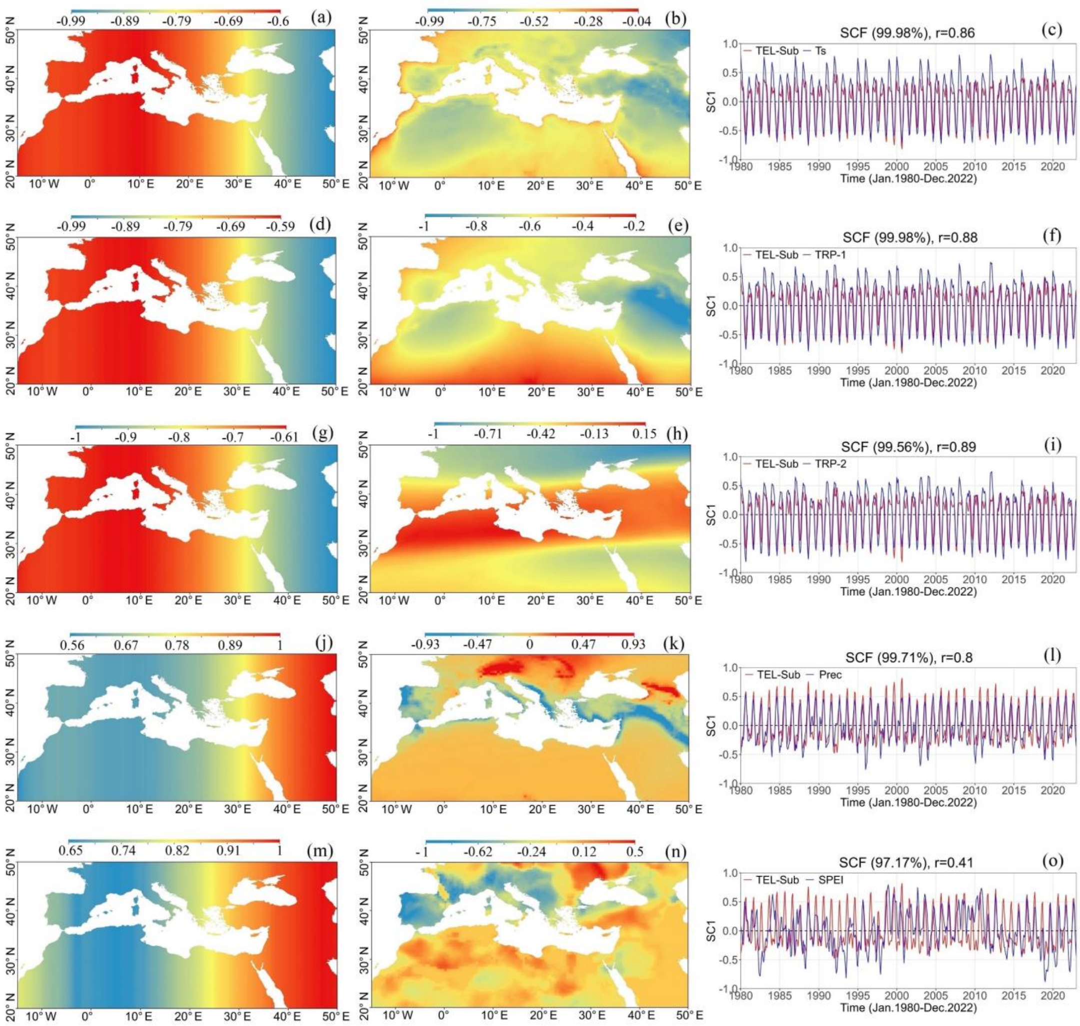

Figure 8. First leading mode of covariability for the coupled fields of TPD TEL and climatic parameters from January 1980 to December 2022. TPD TEL and surface temperature (a, b, c), TPD TEL and lower tropospheric temperature (TRP-1) (d, e, f), TPD TEL and upper tropospheric temperature (TRP-2) (g, h, i), TPD TEL and precipitation (j, k, l), and TPD TEL and SPEI (m, n, o). The spatial patterns for the first paired mode of covariability (SVD1) of TPD TEL (left), climatic parameter SVD1 (middle), and the time series of expansion coefficients (SC1) for the paired mode of both TPD TEL and climatic parameter (right).

https://doi.org/10.5194/egusphere-2025-6521
Preprint. Discussion started: 28 January 2026

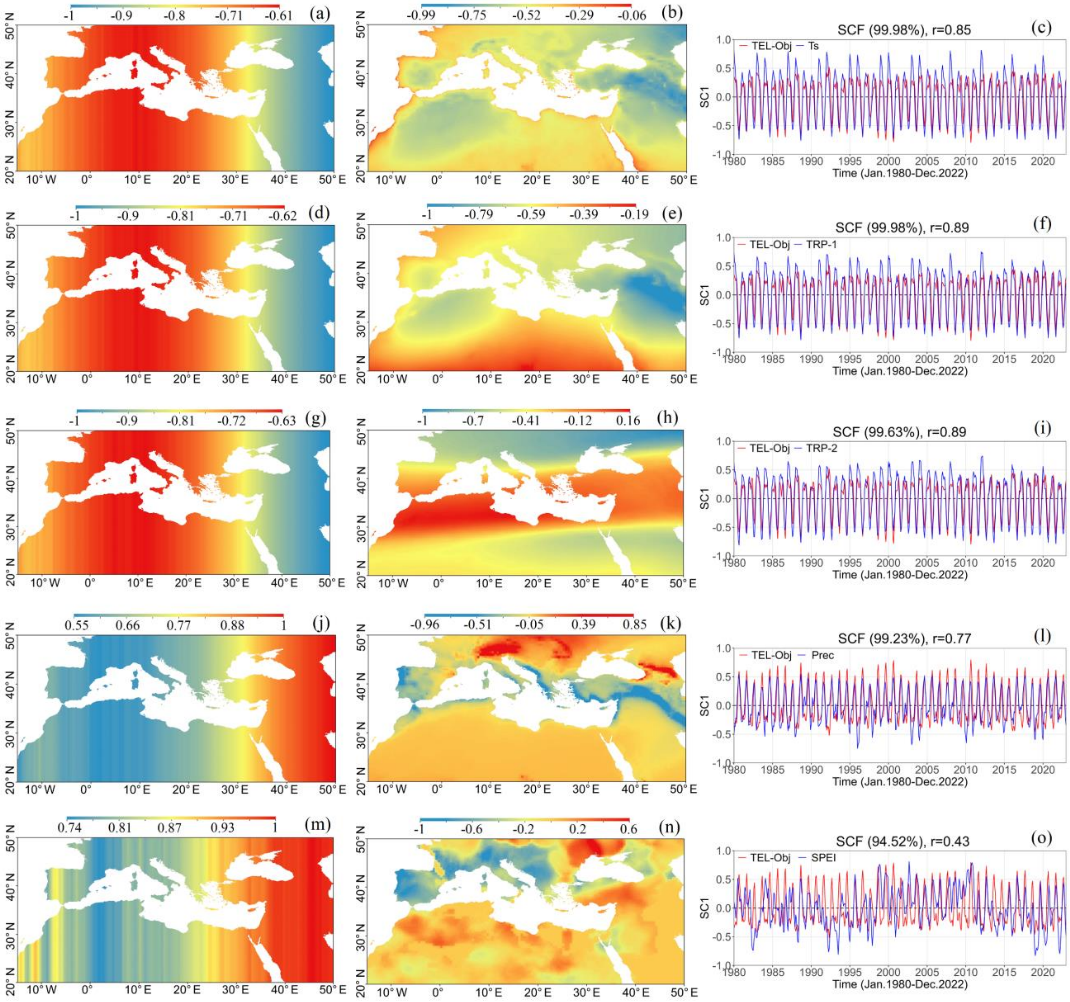

Figure 9. First leading mode of covariability for the coupled fields of TPG TEL and climatic parameters from January 1980 to December 2022. TPG TEL and surface temperature (a, b, c), TPG TEL and lower tropospheric temperature (TRP-1) (d, e, f), TPG TEL and upper tropospheric temperature (TRP-2) (g, h, i), TPG TEL and precipitation (j, k, l), and TPG TEL and SPEI (m, n, o). The spatial patterns for the first paired mode of covariability (SVD1) of TPG TEL (left), climatic parameter SVD1 (middle), and the time series of expansion coefficients (SC1) for the paired mode of both TPG TEL and climatic parameter (right).

The Mediterranean region's monthly average surface temperature over the period from January 1980 to December 2022 has increased by approximately 0.48 ± 0.03 K/dec (Fig. 10a). This is consistent with the results of Castellanos et al. (2021), who found that land surface air temperatures were significantly rising, with yearly amplitudes ranging from 0.006 to 0.027 °C for maximum temperatures and slightly greater rates for minimum temperatures. The primary drivers of Mediterranean region warming are the rapid increase of anthropogenic greenhouse gases and the decline of aerosols and soil moisture (Kim et al., 2019; Urdiales-Flores et al., 2023). Linear regression analysis of surface temperature was performed at all grid points, with decadal trends

https://doi.org/10.5194/egusphere-2025-6521
Preprint. Discussion started: 28 January 2026

plotted (Fig. 10b). Surface temperature shows a dominant upward trend evident across nearly the entire study area, with statistically significant trends at $p < 0.05$ at most of the grid points (Fig. 10b). The greatest temperature upward trends are evident in the eastern Mediterranean region, while temperature trends in the western Mediterranean are less pronounced. Moreover, the zonal mean of the temperature linear regression map on the right panel of Figure 10b shows positive temperature trends throughout the entire study area with maximum trends in the northern zone of the Mediterranean from 46° N to 50° N. Zittis et al. (2022) reported that the Eastern Mediterranean and Middle East are warming approximately twice as rapidly as the global average, indicating that while the Mediterranean as a whole is experiencing dramatic warming, particular locations within it are experiencing far more drastic changes compared to the rest of the globe.

Figure 10c exhibits the monthly time series of Mediterranean TRP-1 for the period from January 1980 to December 2022. TRP-1 has increasing trends of approximately 0.36 ± 0.03 K/dec. The decadal trends of TRP-1 at all grid points over this period (Fig. 10d) show increasing trends, with statistically significant trends at $p < 0.05$ at most of the grid points, caused mainly by global warming. TRP-1 trends in the eastern and northern Mediterranean are much stronger than those in the southern and western Mediterranean, and the zonal mean of TRP-1 linear regression map on the right panel of Figure 10d depicts dominant positive trends throughout the entire study area with the strongest trends in the zone from 45° N to 50° N. For the monthly time series of TRP-2 (Fig. 10e), the decadal trend over the period from January 1980 to December 2022 is 0.09 ± 0.01 K/dec, which is less than that of TRP-1. Additionally, linear regression analysis of TRP-2 performed at all grid points shows clear variation in temperature trends, with statistically significant trends at $p < 0.05$ at most of the grid points. In the northern Mediterranean, positive TRP-2 trends are abundant, while in the southern Mediterranean, negative trends are prevalent (Fig. 10f). The zonal mean of TRP-2 linear regression map on the right panel of Figure 10f displays clear negative trends around the latitude of 31.25° N. Our results are in agreement with Karl et al. (2006), who reported that global-average tropospheric temperatures have increased significantly since the late 20th century. From 1958 to the present, the global average temperature has risen at a rate of approximately 0.12°C per decade, accelerating to about 0.16°C per decade since 1979.

The decadal trends of the monthly zonal mean temperature structure during 1980-2022 over height ranges from the earth's surface to 20 km, including the troposphere and lower stratosphere, and the LRT-H zonal mean is shown in Figure 10g. As evident, there are apparent upward temperature trends in the whole troposphere, with the greatest increasing trends over the latitudinal band from around 45° N-50° N, with a maximum value of 0.5 K/dec. As is clear from the zonal mean of linear regression trend maps of surface temperature, TRP-1, and TRP-2 on the right panel of Figure 10b, d, and f, respectively, there is an observed increase in temperature trends also over the latitudinal band from around 45° N-50° N. The warming in the troposphere is associated with apparent cooling trends in the stratosphere at a greatest rate of slightly over -0.5 K/dec. The latitudinal band 20° N-30° N is the zone of maximum stratospheric temperature declining trends. The phenomenon of tropospheric warming accompanied by stratospheric cooling is a signature fingerprint of human-

https://doi.org/10.5194/egusphere-2025-6521
Preprint. Discussion started: 28 January 2026

induced climate change, principally driven by rising GHGs. Several studies reported tropospheric warming and stratospheric cooling employing radiosonde, radio occultation (RO), and satellite observations (Narayana Rao et al., 2007; Titchner et al., 2009; Haimberger et al., 2012; Steiner et al., 2020).

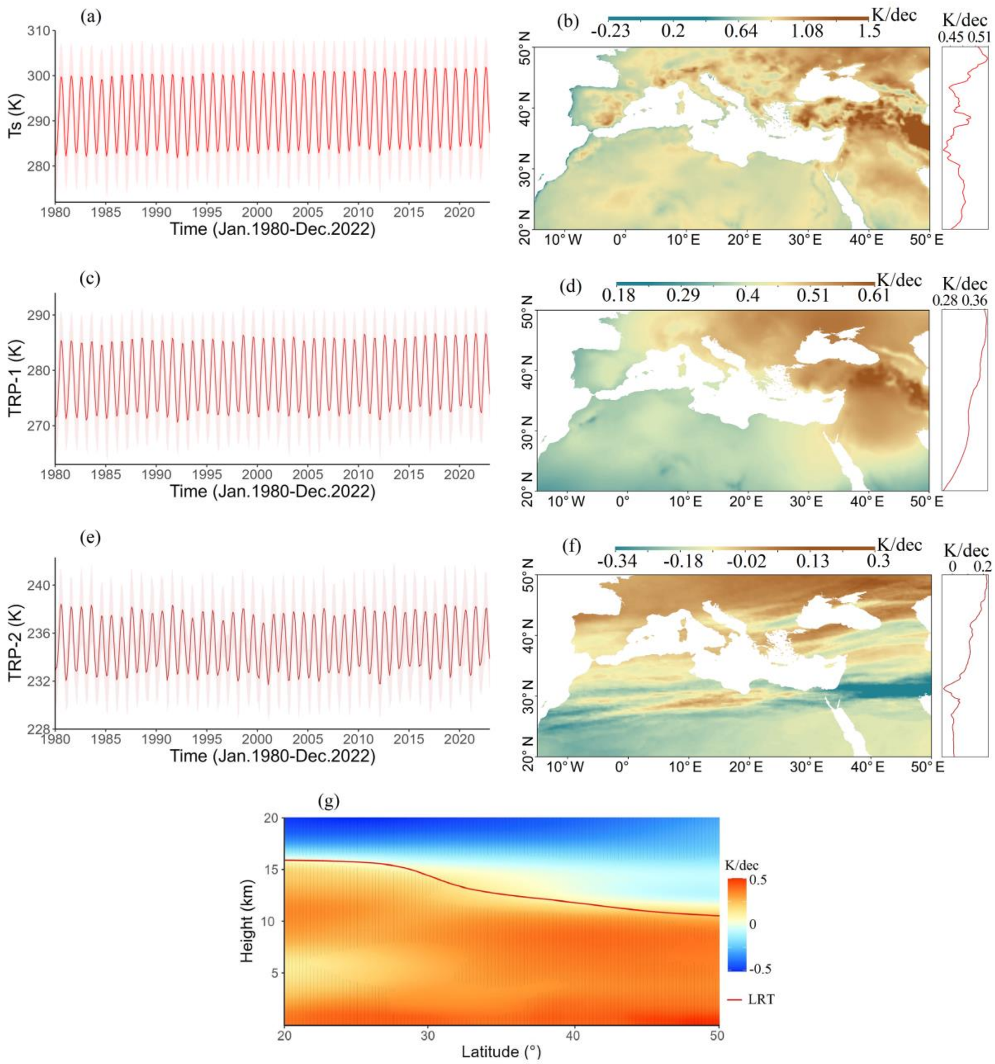

Figure 10. Monthly time series of surface temperature (Ts) (a) and its linear regression analysis at all grid points with decadal trends over the period January 1980 to December 2022, with the zonal mean of the regression map on the right side (b). Monthly time series of lower tropospheric temperature from surface to 5 km height (TRP-1) (c) and its linear regression analysis at all grid points with decadal trends over the period January 1980 to December 2022, with the zonal mean of the regression map on the right side (d). Monthly time series of upper tropospheric temperature from 5 km to LRT level (TRP-2) (e) and its linear regression analysis at all grid points with decadal trends over the period January 1980 to December 2022, with the zonal mean of the regression map on the right side (f). Temperature trends (K/decade) in the troposphere and lower stratosphere (0-20 km) over 1980–2022; the LRT-H is represented by the red line. Dashed lines mark areas where temperature trends are statistically significant at a p-value < 0.05 (g).

https://doi.org/10.5194/egusphere-2025-6521
Preprint. Discussion started: 28 January 2026

Total precipitation over the Mediterranean from January 1980 to December 2022 exhibits decreasing trends of approximately -0.25 ± 0.05 mm/dec (Fig. 11a). This is consistent with previous studies reporting that the Mediterranean region is facing significant changes in precipitation patterns driven by climate change. Observational data and climate model projections indicate a clear trend toward declining precipitation, particularly during winter months, which poses serious implications for the region's ecosystems and water resources (Cos et al., 2022; Delworth et al., 2022; André et al., 2024). Linear regression analysis of total precipitation was performed at all grid points, with decadal trends plotted (Fig. 11b). Precipitation exhibits a dominant downward trend evident in eastern and western Europe, with statistically significant trends at $p < 0.05$ at most of the grid points. Furthermore, the zonal mean of the precipitation linear regression map on the right panel of Figure 11b exhibits evident positive trends around latitude 41° N while depicting a strong negative trend between 47° N and 50° N. SPEI is commonly used to monitor meteorological drought status. As seen in Figure 11c, SPEI has decreased by -0.07 ± 0.001 /dec from January 1980 to December 2022. Recent studies have highlighted significant trends in drought occurrences and characteristics across the Mediterranean Basin (Essa et al., 2023). Historical analyses using SPEI from 1980 to 2014 reveal a significant upward trend in drought frequency (Choutri and Hussien, 2024; Kesgin et al., 2024). SPEI linear regression analysis performed at all grid points exhibits evident abundance of grid cells with decreasing SPEI trends, especially in the northern Mediterranean (Fig. 11d). Additionally, the zonal mean of SPEI, on the right panel of Figure 11d, depicts a strong negative trend between 40° N and 50° N.

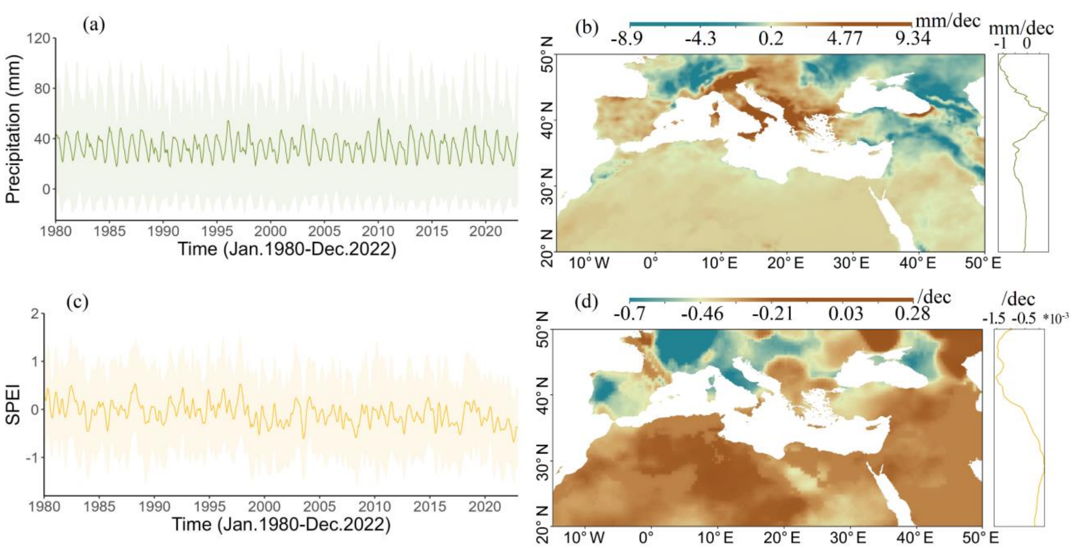

Figure 11. Monthly time series of precipitation (a) and its linear regression analysis at all grid points with decadal trends over the period January 1980 to December 2022, with the zonal mean of the regression map on the right side (b). Monthly time series of Standardized Precipitation Evapotranspiration Index (SPEI) (c) and its linear regression analysis at all grid points with decadal trends over the period January 1980 to December 2022, with the zonal mean of the regression map on the right side (d).

https://doi.org/10.5194/egusphere-2025-6521
Preprint. Discussion started: 28 January 2026

4 Conclusions

The Mediterranean region is increasingly recognized as a climate change hotspot, where the combined impacts of global warming and tropical belt expansion are contributing to significant alterations in climatic patterns. This study investigates the relationship between tropical belt expansion over the Mediterranean region and climatic parameters (tropopause, temperature, precipitation, and SPEI) variations using observational and reanalysis data from January 1980 to December 2022 through comprehensive analyses (correlation, linear regression, SVD, WTC, and PCA). Our findings reveal that monthly average LRT-H increased by approximately 80.58 ± 3.07 m/dec over the study period, attributed to global warming from increasing GHGs emissions (Meng et al., 2021). LRT-H shows stronger positive anomalies than negative ones, while LRT-T displays higher negative anomalies than positive. Moreover, the LRT-H shows dominant upward trends over the study area, which reach maximum values of about 266.5 m/dec in the eastern Mediterranean, reflecting intensifying warming conditions. Our findings corroborate previous research based on GNSS-RO, radiosonde, and reanalysis datasets that have documented rising tropopause height (Schmidt et al., 2004; Sausen and Santer, 2003; Seidel and Randel, 2006; Pisoft et al., 2021). Based on the two used tropopause height metrics, the tropical belt expanded poleward at rates of approximately 0.14 ± 0.05 °/dec and 0.27 ± 0.06 °/dec for TPD and TPG methods, respectively. The tropical belt expansion has long been connected to changes in atmospheric structure caused by global warming. As temperatures increase, enhanced tropospheric warming causes thermal expansion of the troposphere, resulting in a rise in tropopause height. This vertical expansion is accompanied by poleward growth of the area covered by the tropical belt.

TELs exhibit an evident longitudinal variation, as the eastern Mediterranean shows more poleward TEL occurrences compared to that over the western Mediterranean. This east–west contrast is consistent with the stronger influence of subtropical jet variability in the eastern Mediterranean, compared to the greater impact of Atlantic storm tracks in the western Mediterranean (Lionello et al., 2006; Manney et al., 2011). TELs from both methods exhibit strong positive correlations with LRT-H, surface temperature, and tropospheric temperature, while showing strong negative correlations with precipitation. WTC analysis confirms that both TEL definitions are in phase with high coherence to LRT-H, surface temperature, and tropospheric temperature, but out of phase with precipitation. However, no significant relationship exists for SPEI with TELs or other climatic parameters. Spatial correlation analysis reveals that both surface temperature and TRP-1 show positive correlations with TELs across the study area, with the highest values in the eastern Mediterranean. TRP-2 displays predominantly positive spatial correlations with TELs throughout most of the Mediterranean except within the latitudinal band where TELs undergo poleward expansion and equatorward contraction. Precipitation exhibits strong negative spatial correlations with TELs in the eastern Mediterranean while showing positive correlations over southern Europe.

SVD analysis demonstrates that the first mode of temporal variability for paired modes of TELs and all climatic parameters is dominated by inter-annual oscillations. SC1 of TELs shows strong positive correlations with all climatic factors but less in the case of SPEI. The first spatial mode

https://doi.org/10.5194/egusphere-2025-6521
Preprint. Discussion started: 28 January 2026

(SVD1) reveals clear coupling between surface temperature and TRP-1 with TELs in the eastern Mediterranean. For TRP-2, SVD1 shows linkage with TELs in the southernmost and northernmost zones of the study area, while displaying opposite-sign oscillations in southern Europe, northern Africa, and the middle zone of the eastern Mediterranean. Precipitation SVD1 exhibits two strong signals (one in the eastern Mediterranean and another in southern Europe) accompanied by opposite-sign TEL fluctuations over the same regions and another two covariability zones northward of the previous ones but accompanied by TEL fluctuations of the same sign over the same regions. SPEI SVD1 displays clear coupling of the same sign with TELs in major areas of the eastern Mediterranean and northern Africa regions, while in western Europe, both depict opposite sign fluctuations. The stronger coupling between TELs and climatic parameters in the eastern Mediterranean indicates the strong effect of the TEL pattern in this region compared to the broader study area. Surface temperature over the Mediterranean region increased at 0.48 ± 0.03 K/dec between January 1980 and December 2022, with the most significant rises in the eastern Mediterranean and less dramatic increases in the western Mediterranean. TRP-1 and TRP-2 show increasing trends of approximately 0.36 ± 0.03 K/dec and 0.09 ± 0.01 K/dec, respectively, with positive trends most abundant in the eastern and northern Mediterranean for TRP-1 and the northern Mediterranean for TRP-2. The temperature structure across the Mediterranean has the greatest magnitudes and trends near the surface, which gradually drop with altitude and exhibit a strong height-dependent spatial pattern. Total precipitation and SPEI exhibit decreasing trends of approximately -0.25 ± 0.05 mm/dec and -0.07 ± 0.001 /dec, respectively, consistent with previous studies reporting pronounced aridification and more frequent droughts over the Mediterranean region (Essa et al., 2023; André et al., 2024).

These results confirm that climatic parameter variability, coherence, and coupling are linked to TELs variability throughout the Mediterranean region, with apparent interaction and coupling between climatic parameter patterns and TELs over the eastern Mediterranean. The findings of this study advance the understanding of the long-term variability of key climatic parameters over the Mediterranean, as well as their relationships and interactions with large-scale tropical belt dynamics.

Author contribution. Conceptualization: MD and SJ; Methodology: MD; Software: MD; Validation: SJ and MD; Formal analysis: MD; Investigation: SJ and MD; Resources: MD; Data curation: MD; Writing—original draft preparation: MD; Visualization: MD; Writing—review and editing: SJ, MD, AC, AS, IR and AMR; Supervision: SJ.

Competing interests. The authors declare no competing interests.

Acknowledgements. The authors thanks to the Copernicus Climate Change Service Information for ERA5 data. In addition, we are grateful to the Climate Research Unit (CRU), the University of Delaware (UDEL) for granting access to datasets.

Financial support. This study was supported by the National Natural Science Foundation of China (NSFC) Project (Grant No. 12073012).

References

Allen, R. J., Norris, J. R., and Kovilakam, M.: Influence of anthropogenic aerosols and the Pacific Decadal Oscillation on tropical belt width, Nat. Geosci., 7, 270–274, https://doi.org/10.1038/ngeo2091, 2014.

Allen, R. J., Sherwood, S. C., Norris, J. R., and Zender, C. S.: Recent Northern Hemisphere tropical expansion primarily driven by black carbon and tropospheric ozone, Nature, 485, 350–354, https://doi.org/10.1038/nature11097, 2012.

Alpert, P., Price, C., Krichak, S. O., Ziv, B., Saaroni, H., Osetinsky, I., Barkan, J., and Kishcha, P.: Tropical teleconnections to the Mediterranean climate and weather, Adv. Geosci., 2, 157–160, https://doi.org/10.5194/adgeo-2-157-2005, 2005.

André, J., D'Andrea, F., Drobinski, P., and Muller, C.: Regimes of Precipitation Change Over Europe and the Mediterranean, J. Geophys. Res. Atmos., 129, https://doi.org/10.1029/2023JD040413, 2024.

Androulidakis, Y., Makris, C., Mallios, Z., Pytharoulis, I., Baltikas, V., and Krestenitis, Y.: Storm surges and coastal inundation during extreme events in the Mediterranean Sea: the IANOS Medicane, Springer Netherlands, 939–978 pp., https://doi.org/10.1007/s11069-023-05890-6, 2023.

Beguería, S., Vicente-Serrano, S. M., Reig, F., and Latorre, B.: Standardized precipitation evapotranspiration index (SPEI) revisited: Parameter fitting, evapotranspiration models, tools, datasets and drought monitoring, Int. J. Climatol., 34, 3001–3023, https://doi.org/10.1002/joc.3887, 2014.

Bianchi, C. N. and Morri, C.: Global sea warming and "tropicalization" of the Mediterranean Sea: biogeographic and ecological aspects, Biogeogr. – J. Integr. Biogeogr., 24, https://doi.org/10.21426/b6110129, 2003.

Birner, T.: Recent widening of the tropical belt from global tropopause statistics: Sensitivities, J. Geophys. Res. Atmos., 115, 1–13, https://doi.org/10.1029/2010JD014664, 2010.

Bjornsson, H., and Venegas, S. A.: Manual for EOF and SVD analyses of climatic data. Center for Climate and Global Change Research, McGill University, CCGCR Report No. 97-1, Montréal, Québec, 52pp, 1997.

Borghini, M., Bryden, H., Schroeder, K., Sparnocchia, S., and Vetrano, A.: The Mediterranean is becoming saltier, Ocean Sci., 10, 693–700, https://doi.org/10.5194/os-10-693-2014, 2014.

Bronnimann, S., Fischer, A. M., Rozanov, E., Poli, P., Compo, G. P., and Sardeshmukh, P. D.: Southward shift of the northern tropical belt from 1945 to 1980, Nat. Geosci., 8, 969–974, https://doi.org/10.1038/ngeo2568, 2015.

Carlo, N. B., and Morri, C.: Global sea warming and "tropicalization" of the Mediterranean Sea: biogeographic and ecological aspects, Biogeographia – the Journal of Integrative Biogeography, 24. https://doi.org/10.21426/b6110129, 2003.

Castellanos, M., García, M. Á., Pérez, I. A., Sánchez, M. L., Pardo, N., and Fernández-Duque, B.: Measuring temperature trends in the Mediterranean basin, J. Atmos. Solar-Terrestrial Phys., 222, https://doi.org/10.1016/j.jastp.2021.105713, 2021.

Choutri, I. and Hussien, A.: Exploratory Analysis of Algeria Meteorological Drought Using SPI and SPEI, OALib, 11, 1–27, https://doi.org/10.4236/oalib.1111897, 2024.

Coll, M., Piroddi, C., Steenbeek, J., Kaschner, K., Lasram, F. B. R., Aguzzi, J., Ballesteros, E., Bianchi, C. N., Corbera, J., Dailianis, T., Danovaro, R., Estrada, M., Froglia, C., Galil, B. S., Gasol, J. M., Gertwage, R., Gil, J., Guilhaumon, F., Kesner-Reyes, K., Kitsos, M. S., Koukouras, A., Lampadariou, N., Laxamana, E., de la Cuadra, C. M. L. F., Lotze, H. K., Martin, D., Mouillot, D., Oro, D., Raicevich, S., Rius-Barile, J., Saiz-Salinas, J. I., Vicente, C. S., Somot, S., Templado, J., Turon, X., Vafidis, D., Villanueva, R., and Voultsiadou, E.: The biodiversity of the Mediterranean Sea: Estimates, patterns, and threats, PLoS One, 5, https://doi.org/10.1371/journal.pone.0011842, 2010.

Cos, J., Doblas-Reyes, F., Jury, M., Marcos, R., Bretonnière, P. A., and Samsó, M.: The Mediterranean climate change hotspot in the CMIP5 and CMIP6 projections, Earth Syst. Dyn., 13, 321–340, https://doi.org/10.5194/esd-13-321-2022, 2022.

Cramer, W., Guiot, J., Fader, M., Garrabou, J., Gattuso, J. P., Iglesias, A., Lange, M. A., Lionello, P., Llasat, M. C., Paz, S., Peñuelas, J., Snoussi, M., Toreti, A., Tsimplis, M. N., and Xoplaki, E.: Climate change and interconnected risks to sustainable development in the Mediterranean, Nat. Clim. Chang., 8, 972–980, https://doi.org/10.1038/s41558-018-0299-2, 2018.

Darrag, M.: Global Climate Change Detection Using GNSS Radio Occultation, PhD thesis. Nanjing University of Information Science &Technology. China, 2024.

Darrag, M., Jin, S., Calabia, A., and Samy, A.: Determination of tropical belt widening using multiple GNSS radio occultation measurements, Ann. Geophys., 40, 359–377, https://doi.org/10.5194/angeo-40-359-2022, 2022.

Darrag, M., Jin, S., and Samy, A.: Effect of global gravity wave activity on tropopause variation characteristics from multiple GNSS-RO observations, Theor. Appl. Climatol., 155, 2669–2688, https://doi.org/10.1007/s00704-023-04780-y, 2024.

Davis, N. A. and Birner, T.: Seasonal to multidecadal variability of the width of the tropical belt, J. Geophys. Res. Atmos., 118, 7773–7787, https://doi.org/10.1002/jgrd.50610, 2013.

Davis, N. and Birner, T.: On the discrepancies in tropical belt expansion between reanalyses and climate models and among tropical belt width metrics, J. Clim., 30, 1211–1231, https://doi.org/10.1175/JCLI-D-16-0371.1, 2017.

Davis, S. M. and Rosenlof, K. H.: A multidiagnostic intercomparison of tropical-width time series using reanalyses and satellite observations, J. Clim., 25, 1061–1078, https://doi.org/10.1175/JCLI-D-11-00127.1, 2012.

Delworth, T. L., Cooke, W. F., Naik, V., Paynter, D., and Zhang, L.: A weakened AMOC may prolong greenhouse gas–induced Mediterranean drying even with significant and rapid climate change mitigation, Proc. Natl. Acad. Sci. U. S. A., 119, 1–8, https://doi.org/10.1073/pnas.2116655119, 2022.

Essa, Y. H., Hirschi, M., Thiery, W., El-Kenawy, A. M., and Yang, C.: Drought characteristics in Mediterranean under future climate change, npj Clim. Atmos. Sci., 6, 25–28, https://doi.org/10.1038/s41612-023-00458-4, 2023.

Faugeras, B., Bernard, O., Sciandra, A., and Lévy, M.: A mechanistic modelling and data assimilation approach to estimate the carbon/chlorophyll and carbon/nitrogen ratios in a coupled hydrodynamical-biological model, Nonlinear Process. Geophys., 11, 515–533, https://doi.org/10.5194/npg-11-515-2004, 2004.

Gao, X. and Giorgi, F.: Increased aridity in the Mediterranean region under greenhouse gas forcing estimated from high resolution simulations with a regional climate model, Glob. Planet. Change, 62, 195–209, https://doi.org/10.1016/j.gloplacha.2008.02.002, 2008.

https://doi.org/10.5194/egusphere-2025-6521
Preprint. Discussion started: 28 January 2026

Giorgi, F.: Climate change hot-spots, Geophys. Res. Lett., 33, 1–4, https://doi.org/10.1029/2006GL025734, 2006.

Giorgi, F.: Thirty Years of Regional Climate Modeling: Where Are We and Where Are We Going next?, J. Geophys. Res. Atmos., 124, 5696–5723, https://doi.org/10.1029/2018JD030094, 2019.

Gnanadesikan, A. and Stouffer, R. J.: Diagnosing atmosphere-ocean general circulation model errors relevant to the terrestrial biosphere using the Köppen climate classification, Geophys. Res. Lett., 33, 1–5, https://doi.org/10.1029/2006GL028098, 2006.

Grinsted, A., Moore, J. C., and Jevrejeva, S.: Application of the cross wavelet transform and wavelet coherence to geophysical time series, Nonlinear Processes in Geophysics, 11(5/6), 561–566. https://doi.org/10.5194/npg-11-561-2004, 2004.

Grise, K. M., Davis, S. M., Staten, P. W., and Adam, O.: Regional and seasonal characteristics of the recent expansion of the tropics, J. Clim., 31, 6839–6856, https://doi.org/10.1175/JCLI-D-18-0060.1, 2018.

Haimberger, L., Tavolato, C., and Sperka, S.: Homogenization of the global radiosonde temperature dataset through combined comparison with reanalysis background series and neighboring stations, J Climate 25:8108–8131, https:// doi. org/ 10. 1175/ JCLI-D- 11- 00668.1, 2012.

Harris, I., Osborn, T. J., Jones, P., and Lister, D.: Version 4 of the CRU TS monthly high-resolution gridded multivariate climate dataset, Sci. Data, 7, 1–18, https://doi.org/10.1038/s41597-020-0453-3, 2020.

Hersbach, H., Bell, B., Berrisford, P., Biavati, G., Horányi, A., Muñoz Sabater, J., Nicolas, J., Peubey, C., Radu, R., Rozum, I., Schepers, D., Simmons, A., Soci, C., Dee, D., and Thépaut, J.- N.: ERA5 monthly averaged data on pressure levels from 1979 to present, Copernicus Climate Change Service (C3S) Climate Data Store (CDS) [data set], https://doi.org/10.24381/cds.6860a573, 2019a.

Hersbach, H., Bell, B., Berrisford, P., Biavati, G., Horányi, A., Muñoz Sabater, J., Nicolas, J., Peubey, C., Radu, R., Rozum, I., Schepers, D., Simmons, A., Soci, C., Dee, D., and Thépaut, J.- N.: ERA5 monthly averaged data on single levels from 1979 to present, Copernicus Climate Change Service (C3S) Climate Data Store (CDS) [data set], https://doi.org/10.24381/cds.f17050d7, 2019b.

Hindley, N. P., Wright, C. J., Smith, N. D., and Mitchell, N. J.: The southern stratospheric gravity wave hot spot: Individual waves and their momentum fluxes measured by COSMIC GPS-RO, Atmos. Chem. Phys., 15, 7797–7818, https://doi.org/10.5194/acp-15-7797-2015, 2015.

Insua-Costa, D., Senande-Rivera, M., Llasat, M. C., and Miguez-Macho, G.: A global perspective on western Mediterranean precipitation extremes, npj Clim. Atmos. Sci., 5, 1–7, https://doi.org/10.1038/s41612-022-00234-w, 2022.

IPCC.: Climate Change 2021: Impacts, Adaptation and Vulnerability. Contribution of Working Group II to the Sixth Assessment Report of the Intergovernmental Panel on Climate Change, Cambridge University Press, https://www.ipcc.ch/report/ar6/wg2/, 2021a.

IPCC.: Climate change 2021: The physical science basis. Contribution of Working Group I to the Sixth Assessment Report of the Intergovernmental Panel on Climate Change, Cambridge University Press, https://doi.org/10.1017/9781009157896, 2021b.

Karl, T. R., Hassol, S. J., Miller, C. D., and Murray, W. L.: Temperature trends in the lower Atmosphere: Steps for understanding and reconciling differences, U.S. Climate Change Science Program eBooks. Retrieved from https://digital.library.unt.edu/ark:/67531/metadc12017/m2/1/high_res_d/sap1-1-final-all.pdf, 2006.

https://doi.org/10.5194/egusphere-2025-6521
Preprint. Discussion started: 28 January 2026

Kesgin, E., Yaldız, S. G., and Güçlü, Y. S.: Spatiotemporal variability and trends of droughts in the Mediterranean coastal region of Türkiye, International Journal of Climatology. 44(4), 1036–1057. https://doi.org/10.1002/joc.8370, 2024.

Kim, G. U., Seo, K. H., and Chen, D.: Climate change over the Mediterranean and current destruction of marine ecosystem, Sci. Rep., 9, 1–9, https://doi.org/10.1038/s41598-019-55303-7, 2019.

Kuglitsch, F. G., Toreti, A., Xoplaki, E., Della-Marta, P. M., Zerefos, C. S., Trke, M., and Luterbacher, J.: Heat wave changes in the eastern mediterranean since 1960, Geophys. Res. Lett., 37, 1–5, https://doi.org/10.1029/2009GL041841, 2010.

Lange, M. A.: Climate Change in the Mediterranean: Environmental Impacts and Extreme Events, IEMed Mediterr. Yearb., 1–12, 2020.

Lionello, P., Abrantes, F., Gualdi, S., et al.: Introduction: The climate of the Mediterranean region, Elsevier eBooks. https://doi.org/10.1016/c2011-0-06210-5, 2012.

Lionello, P., Malanotte-Rizzoli, P., Boscolo, R., Alpert, P., Artale, V., Li, L., . . . Xoplaki, E.: The Mediterranean climate: An overview of the main characteristics and issues, In Developments in earth and environmental sciences (pp. 1–26). https://doi.org/10.1016/s1571-9197(06)80003-0, 2006.

Luan, L., Staten, P. W., Chi, O. A. O., and Qiang, F. U.: Seasonal and annual changes of the regional tropical belt in GPS-RO measurements and reanalysis datasets, J. Clim., 33, 4083–4094, https://doi.org/10.1175/JCLI-D-19-0671.1, 2020.

Lucas, C., Timbal, B., and Nguyen, H.: The expanding tropics: A critical assessment of the observational and modeling studies, Wiley Interdiscip. Rev. Clim. Chang., 5, 89–112, https://doi.org/10.1002/wcc.251, 2014.

Luterbacher, J., Xoplaki, E., Casty, C., Wanner, H., Pauling, A., Küttel, M., Rutishauser, T., Brönnimann, S., Fischer, E., Fleitmann, D., Gonzalez-Rouco, F. J., García-Herrera, R., Barriendos, M., Rodrigo, F., Gonzalez-Hidalgo, J. C., Saz, M. A., Gimeno, L., Ribera, P., Brunet, M., Paeth, H., Rimbu, N., Felis, T., Jacobeit, J., Dünkeloh, A., Zorita, E., Guiot, J., Türkes, M., Alcoforado, M. J., Trigo, R., Wheeler, D., Tett, S., Mann, M. E., Touchan, R., Shindell, D. T., Silenzi, S., Montagna, P., Camuffo, D., Mariotti, A., Nanni, T., Brunetti, M., Maugeri, M., Zerefos, C., Zolt, S. De, Lionello, P., Nunes, M. F., Rath, V., Beltrami, H., Garnier, E., and Ladurie, E. L. R.: Chapter 1 Mediterranean climate variability over the last centuries: A review, Dev. Earth Environ. Sci., 4, 27–148, https://doi.org/10.1016/S1571-9197(06)80004-2, 2006.

Manney, G. L., Hegglin, M. I., Daffer, W. H., Santee, M. L., Ray, E. A., Pawson, S., Schwartz, M. J., Boone, C. D., Froidevaux, L., Livesey, N. J., Read, W. G., and Walker, K. A.: Jet characterization in the upper troposphere/lower stratosphere (UTLS): Applications to climatology and transport studies, Atmos. Chem. Phys., 11, 6115–6137, https://doi.org/10.5194/acp-11-6115-2011, 2011.

Mastrorillo, M., Scartozzi, C. M., Pacillo, G., Menza, G., Desai, B., Maviza, G., Jaskolski, M., Schapendonk, F., Meddings, G., and Carneiro, B.: Towards a common vision for climate change, security and migration in the Mediterranean, 2024.

Mathew, S. S. and Kumar, K. K.: Estimation of zonally resolved edges of the tropical belt using GPS-RO measurements, IEEE J. Sel. Top. Appl. Earth Obs. Remote Sens., 11, 2555–2561, https://doi.org/10.1109/JSTARS.2018.2828342, 2018.

Meli, M., Camargo, C. M. L., Olivieri, M., Slangen, A. B. A., and Romagnoli, C.: Sea-level trend variability in the Mediterranean during the 1993–2019 period, Front. Mar. Sci., 10, 1–18, https://doi.org/10.3389/fmars.2023.1150488, 2023.

https://doi.org/10.5194/egusphere-2025-6521
Preprint. Discussion started: 28 January 2026

Meng, L., Liu, J., Tarasick, D. W., Randel, W. J., Steiner, A. K., Wilhelmsen, H., Wang, L., and Haimberger, L.: Continuous rise of the tropopause in the Northern Hemisphere over 1980–2020, Sci. Adv., 7, 1–9, https://doi.org/10.1126/sciadv.abi8065, 2021.

Miller, C. D.: Temperature Trends in the Lower Atmosphere Steps for Understanding and, Program, 17, 180, 2006.

Minh, H. V. T., Lien, B. T. B., Hong Ngoc, D. T., Ty, T. Van, Ngan, N. V. C., Cong, N. P., Downes, N. K., Meraj, G., and Kumar, P.: Understanding Rainfall Distribution Characteristics over the Vietnamese Mekong Delta: A Comparison between Coastal and Inland Localities, Atmosphere (Basel)., 15, https://doi.org/10.3390/atmos15020217, 2024.

Noto, L. V., Cipolla, G., Pumo, D., and Francipane, A.: Climate Change in the Mediterranean Basin (Part II): A Review of Challenges and Uncertainties in Climate Change Modeling and Impact Analyses, Water Resour. Manag., 37, 2307–2323, https://doi.org/10.1007/s11269-023-03444-w, 2023.

Pisoft, P., Sacha, P., Polvani, L. M., Añel, J. A., De La Torre, L., Eichinger, R., Foelsche, U., Huszar, P., Jacobi, C., Karlicky, J., Kuchar, A., Miksovsky, J., Zak, M., and Rieder, H. E.: Stratospheric contraction caused by increasing greenhouse gases, Environ. Res. Lett., 16, https://doi.org/10.1088/1748-9326/abfe2b, 2021.

Post, D. A., Timbal, B., Chiew, F. H. S., Hendon, H. H., Nguyen, H., and Moran, R.: Decrease in southeastern Australian water availability linked to ongoing Hadley cell expansion, Earth's Futur., 2, 231–238, https://doi.org/10.1002/2013ef000194, 2014.

Raihan, A.: A review of the global climate change impacts, adaptation strategies, and mitigation options in the socio-economic and environmental sectors, J. Environ. Sci. Econ., 2, 36–58, https://doi.org/10.56556/jescae.v2i3.587, 2023.

Narayana Rao, D., Venkat Ratnam, M., Krishna Murthy, B. V., Jagannadha Rao, V. V. M., Kumar Mehta, S., Nath, D., and Ghouse Basha, S.: Identification of tropopause using bending angle profile from GPS radio occultation (RO): A radio tropopause, Geophys. Res. Lett., 34, 1–7, https://doi.org/10.1029/2007GL029709, 2007.

Rilov, G. and Crooks, J. A.: Biological Invasions in Marine Ecosystems, 641 pp. pp., 2009.

Santer, B. D., Wigley, T. M. L., Simmons, A. J., Kållberg, P. W., Kelly, G. A., Uppala, S. M., Ammann, C., Boyle, J. S., Brüggemann, W., Doutriaux, C., Fiorino, M., Mears, C., Meehl, G. A., Sausen, R., Taylor, K. E., Washington, W. M., Wehner, M. F., and Wentz, F. J.: Identification of anthropogenic climate change using a second-generation reanalysis, J. Geophys. Res. D Atmos., 109, 1–19, https://doi.org/10.1029/2004JD005075, 2004.

Sausen, R. and Santer, B. D.: Use of changes in tropopause height to detect human influences on climate, Meteorol. Zeitschrift, 12, 131–136, https://doi.org/10.1127/0941-2948/2003/0012-0131, 2003.

Schmidt, D. F. and Grise, K. M.: The Response of Local Precipitation and Sea Level Pressure to Hadley Cell Expansion, Geophys. Res. Lett., 44, 10,573-10,582, https://doi.org/10.1002/2017GL075380, 2017.

Schmidt, T., Wickert, J., Beyerle, G., and Heise, S.: Global tropopause height trends estimated from GPS radio occultation data, Geophys. Res. Lett., 35, 1–5, https://doi.org/10.1029/2008GL034012, 2008.

Schmidt, T., Wickert, J., Beyerle, G., and Reigber, C.: Tropical tropopause parameters derived from GPS radio occultation measurements with CHAMP, J. Geophys. Res. D Atmos., 109, 1–13, https://doi.org/10.1029/2004JD004566, 2004.

Seidel, D. J., Fu, Q., Randel, W. J., and Reichler, T. J.: Widening of the tropical belt in a changing climate, Nature Geoscience, 1(1), 21–24, https://doi.org/10.1038/ngeo.2007.38, 2008.

https://doi.org/10.5194/egusphere-2025-6521
Preprint. Discussion started: 28 January 2026

Seidel, D. J. and Randel, W. J.: Variability and trends in the global tropopause estimated from radiosonde data, J. Geophys. Res. Atmos., 111, 1–17, https://doi.org/10.1029/2006JD007363, 2006.

Seidel, D. J., Ross, R. J., Angell, J. K., and Reid, G. C.: Climatological characteristics of the tropical tropopause as revealed by radiosondes, J. Geophys. Res. Atmos., 106, 7857–7878, https://doi.org/10.1029/2000JD900837, 2001.

Somot, S., Sevault, F., and Déqué, M.: Transient climate change scenario simulation of the Mediterranean Sea for the twenty-first century using a high-resolution ocean circulation model, Clim. Dyn., 27, 851–879, https://doi.org/10.1007/s00382-006-0167-z, 2006.

Staten, P. W., Lu, J., Grise, K. M., Davis, S. M., and Birner, T.: Re-examining tropical expansion, Nat. Clim. Chang., 8, 768–775, https://doi.org/10.1038/s41558-018-0246-2, 2018.

Steiner, A. K., Ladstädter, F., Randel, W. J., Maycock, A. C., Fu, Q., Claud, C., Gleisner, H., Haimberger, L., Ho, S. P., Keckhut, P., Leblanc, T., Mears, C., Polvani, L. M., Santer, B. D., Schmidt, T., Sofieva, V., Wing, R., and Zou, C. Z.: Observed temperature changes in the troposphere and stratosphere from 1979 to 2018, J. Clim., 33, 8165–8194, https://doi.org/10.1175/JCLI-D-19-0998.1, 2020.

Trigo, R., Xoplaki, E., Zorita, E., and Luterbacher, J.: Relations between Variability in the Mediterranean Region and Mid-Latitude Variability, Mediterr. Clim. Var., 179–226, 2006.

Titchner, H. A., Thorne, P. W., McCarthy, M. P., Tett, S. F. B., Haimberger, L., and Parker, D. E.: Critically reassessing tropospheric temperature trends from radiosondes using realistic validation experiments, J. Clim., 22, 465–485, https://doi.org/10.1175/2008JCLI2419.1, 2009.

Tyrlis, E. and Lelieveld, J.: Climatology and dynamics of the summer Etesian winds over the eastern Mediterranean, J. Atmos. Sci., 70, 3374–3396, https://doi.org/10.1175/JAS-D-13-035.1, 2013.

Ulbrich, U., May, W., Li, L., Lionello, P., Pinto, J. G., and Somot, S.: Chapter 8 The Mediterranean climate change under global warming, Dev. Earth Environ. Sci., 4, 399–415, https://doi.org/10.1016/S1571-9197(06)80011-X, 2006.

Urdiales-Flores, D., Zittis, G., Hadjinicolaou, P., Osipov, S., Klingmüller, K., Mihalopoulos, N., Kanakidou, M., Economou, T., and Lelieveld, J.: Drivers of accelerated warming in Mediterranean climate-type regions, npj Clim. Atmos. Sci., 6, https://doi.org/10.1038/s41612-023-00423-1, 2023.

Vicente-Serrano, S. M., Beguería, S., and López-Moreno, J. I.: A multiscalar drought index sensitive to global warming: The standardized precipitation evapotranspiration index, J. Clim., 23, 1696–1718, https://doi.org/10.1175/2009JCLI2909.1, 2010.

Vicente-Serrano, S. M., Tramblay, Y., Reig, F., González-Hidalgo, J. C., Beguería, S., Brunetti, M., Kalin, K. C., Patalen, L., Kržič, A., Lionello, P., Lima, M. M., Trigo, R. M., El-Kenawy, A. M., Eddenjal, A., Türkes, M., Koutroulis, A., Manara, V., Maugeri, M., Badi, W., Mathbout, S., Bertalanič, R., Bocheva, L., Dabanli, I., Dumitrescu, A., Dubuisson, B., Sahabi-Abed, S., Abdulla, F., Fayad, A., Hodzic, S., Ivanov, M., Radevski, I., Peña-Angulo, D., Lorenzo-Lacruz, J., Domínguez-Castro, F., Gimeno-Sotelo, L., García-Herrera, R., Franquesa, M., Halifa-Marín, A., Adell-Michavila, M., Noguera, I., Barriopedro, D., Garrido-Perez, J. M., Azorin-Molina, C., Andres-Martin, M., Gimeno, L., Nieto, R., Llasat, M. C., Markonis, Y., Selmi, R., Ben Rached, S., Radovanović, S., Soubeyroux, J. M., Ribes, A., Saidi, M. E., Bataineh, S., El Khalki, E. M., Robaa, S., Boucetta, A., Alsafadi, K., Mamassis, N., Mohammed, S., Fernández-Duque, B., Cheval, S., Moutia, S., Stevkov, A., Stevkova, S., Luna, M. Y., and Potopová, V.: High temporal variability not trend dominates Mediterranean precipitation, Nature, 639, 658–666, https://doi.org/10.1038/s41586-024-08576-6, 2025.

WMO: Meteorology – A three dimensional science: Second session of the commission for aerology, WMO Bull. 4, WMO – World Meteorological Organization, Geneva, https://library. wmo.int/idurl/4/42003, 1957.

Yavaşlı, D. D. and Erlat, E.: Tropical nights in the Mediterranean: A spatiotemporal analysis of trends from 1950 to 2022, Int. J. Climatol., 44, 1472–1488, https://doi.org/10.1002/joc.8394, 2024.

Zittis, G., Almazroui, M., Alpert, P., Ciais, P., Cramer, W., Dahdal, Y., Fnais, M., Francis, D., Hadjinicolaou, P., Howari, F., Jrrar, A., Kaskaoutis, D. G., Kulmala, M., Lazoglou, G., Mihalopoulos, N., Lin, X., Rudich, Y., Sciare, J., Stenchikov, G., Xoplaki, E., and Lelieveld, J.: Climate Change and Weather Extremes in the Eastern Mediterranean and Middle East, Rev. Geophys., 60, https://doi.org/10.1029/2021RG000762, 2022.